Normal conducting, High Repetition Rate C-band Injectors as Drivers of Radiation Sources and High Gradient Accelerators

Anna Giribono

INFN-LNF

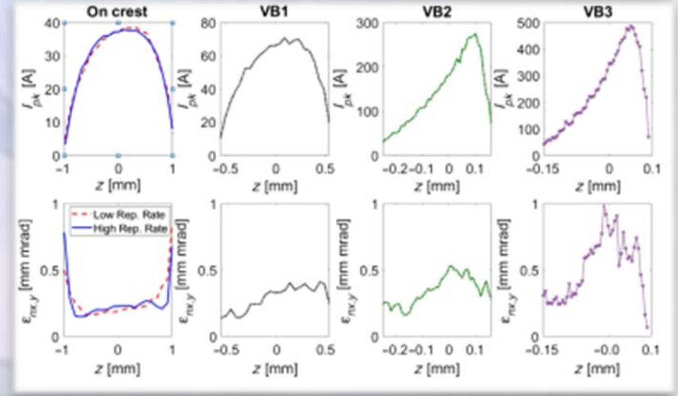

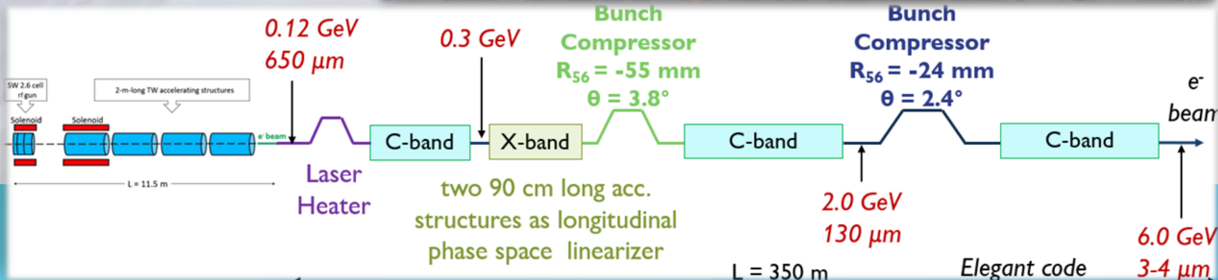

OUTLINE

- RF Injectors as Drivers of Radiation Sources and High Gradient Accelerators
- Normal conducting, high repetition rate C-band injectors for high brightness beam applications
- Applications
  - ICS X-ray source - BoCXS
  - X-ray FEL - EuRIZON/CremlinPlus
  - PWFA stage - EuPRAXIA
- Summary

RF Injectors as Drivers of Radiation Sources and High Gradient Accelerators

[1] ICS X-ray source - BoCXS

high phase space density, high charge, low emittance intended as projected quantities.
Low energy spread → high spectral density and/or monochromaticity

$$N_\gamma^{bw} = \frac{4.1 \times 10^8 U_L[\mathrm{J}] Q_b[pC] \Psi^2}{h\upsilon_l[\mathrm{eV}]\left(\sigma_x^2[\mu\mathrm{m}] + \frac{W_0^2}{4}\right)}$$

$$\frac{\Delta\upsilon_\gamma}{\upsilon_\gamma} = \sqrt{(\gamma\theta)_{\mathrm{rms}}{}^4 + \left(\frac{\Delta\gamma}{\gamma}\right)^2 + \left(\frac{\varepsilon_n}{\sigma_x}\right)^4 + \ldots}$$

Acceptance Angle

X-ray FEL - EuRIZON/CremlinPlus [2]

high intensity phase space → high peak current, low emittance and energy spread intended as **slice** quantities

$$\rho = \frac{1}{4\pi\gamma}\sqrt[3]{2\pi\frac{J}{I_0}\left(\lambda_u K f_b(K)\right)^2}$$

$$\frac{\Delta\omega}{\omega} \approx \rho \qquad \text{and} \qquad P_S \simeq \sqrt{2}\rho P$$

$$L_g = \frac{\lambda_u}{4\pi\sqrt{3}\rho}.$$

$$L_S \simeq 1.066 L_g \ln\left(\frac{9P_S}{P_0}\right)$$

PWFA stage - EuPRAXIA [3]

longitudinal and transverse dimensions in the micrometer range → high intensity phase space intended as rms quantities

$$k_p = \frac{2\pi}{\lambda_p} = \sqrt{\frac{e^2 n_0}{\varepsilon_0 m_e c^2}}$$

$$\beta_x = \frac{2\sqrt{\gamma}}{k_p} \qquad k_p\sigma_z = \sqrt{2}$$

Brightness as beam quality factor

$$B[\mathrm{A/m^2}] = \frac{Q}{\varepsilon_{nx}\varepsilon_{ny}\sigma_t\sigma_\gamma},$$

[1] O. Adriani et al.'Technical Design Report EuroGammaS proposal for the ELI-NP Gamma beam System' (2014) Editor L. Serafini - https://arxiv.org/abs/1407.3669
[2] Assmann, R.W., Weikum, M.K., Akhter, T. et al. EuPRAXIA Conceptual Design Report. Eur. Phys. J. Spec. Top. (2020). https://doi.org/10.1140/epjst/e2020-000127-8
[3] D. Alesini et al. 'EuPRAXIA@SPARC_LAB CDR' – Editor M. Ferrario, Report number: INFN-18-03/LNF (2018)

Normal conducting, high repetition rate C-band injectors for high brightness beam applications

- The aim is to enable higher repetition rate operation and beam performances with respect to the state of the art

→ ***vantage: compactness, beam brightness and flux***

- The C-band technology represents a good compromise between the S and X-band ones

✓ it still allows for exploring a wide range in terms of beam charge and length

✓ Higher achievable cathode, and cavity peak field as high as 160-180 MV/m and 40 MV/m → higher beam brightness

✓ it allows for a more compact beamline compared to S-band solution

✓ Higher efficiency, so it enables high repetition rate operation with higher field compered to S-band solution

→ up to 160 MV/m peak field on cathode in the gun (@400Hz)

→15 MV/m average field in TW sections (@400Hz)

- **Reduced injector footprint by increasing high-quality high-brightness beams and source flux**

The C-band RF photoinjector

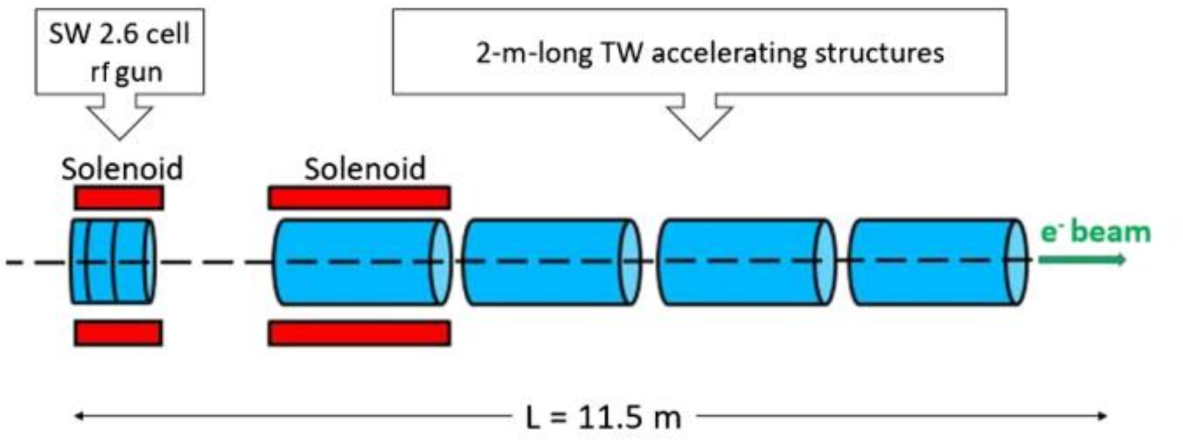

- The C-band photoinjector has been designed in the framework of the XLS, IFAST and EuPRAXIa collaboration.
- It enables the production of electron beams with brightness of the order of 10^3 TAm^2 that turns in transverse emittance lower than 1 mm-mrad and final kA peak current

TABLE I. List of the working points described in this paper. [13]

[4,5]

	Low charge (XLS)		Medium charge			High charge		Units
Charge	75	75	200	200	200	500	500	pC
Average energy	125	105	125	250	200	200	125	MeV
Transverse normalized emittance (100%—rms)	0.15	0.18	0.25	0.25	0.37–0.69	1.3	0.65	mm mrad
Transverse normalized emittance (95%—rms)	0.11	0.13	0.18	0.16	0.25–0.45	0.80	0.44	mm mrad
Length (rms)	380	100	500	500	280–55	55	720	µm
Peak current	20	85	40	40	70–500	1000	70	Ampere
rf compression	off	on	off	off	on	on	off	
Repetition Rate	high	high	high	low	low	low	high	
Peak field @cathode	160	160	160	180	180	180	160	MV/m
TW structure accelerating field	15	15	15	31	31	31	15	MV/m

[4] Compact-Light Design Study (G. D'Auria et al, doi:10.18429/JACoW-IPAC2019-TUPRB032)
[5] Giribono et al. - Dynamics studies of high brightness electron beams in a normal conducting, high repetition rate C-band injector, PRAB 26, 083402 (2023)

Beam dynamics studies

$$\frac{\Delta\gamma}{\gamma} \approx 2\left(\frac{\pi f_{RF}\sigma_z}{c}\right)^2$$

- The beam dynamics has been studied to generate beams with variable charge and length with lowest emittance as possible
- Both velocity bunching (VB) and on-crest operation have been evaluated

[5]

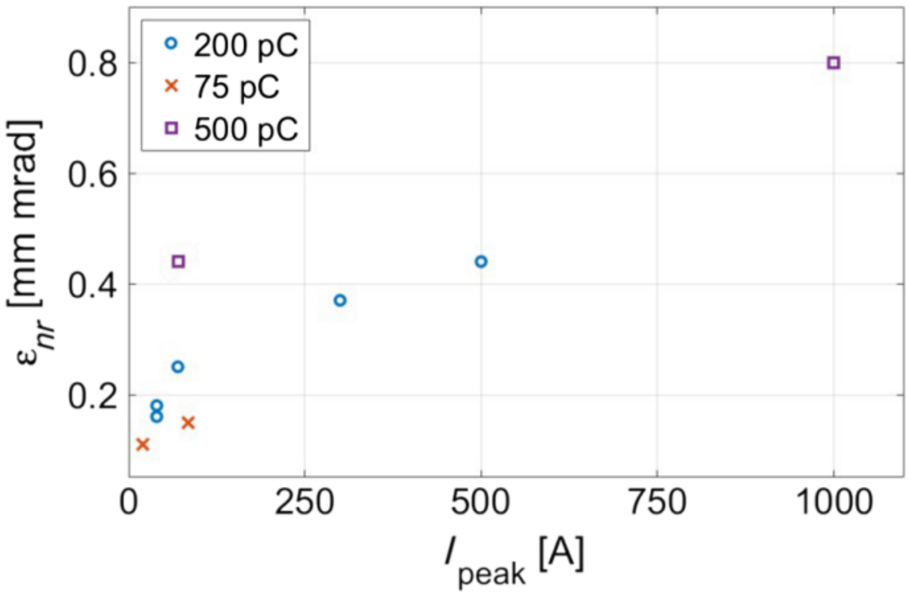

very close to the SwissFEL facility

Suitable to avoid distortions of the longitudinal phase space in a downstream X or C-band booster linac, respectively.

driver of a PWFA

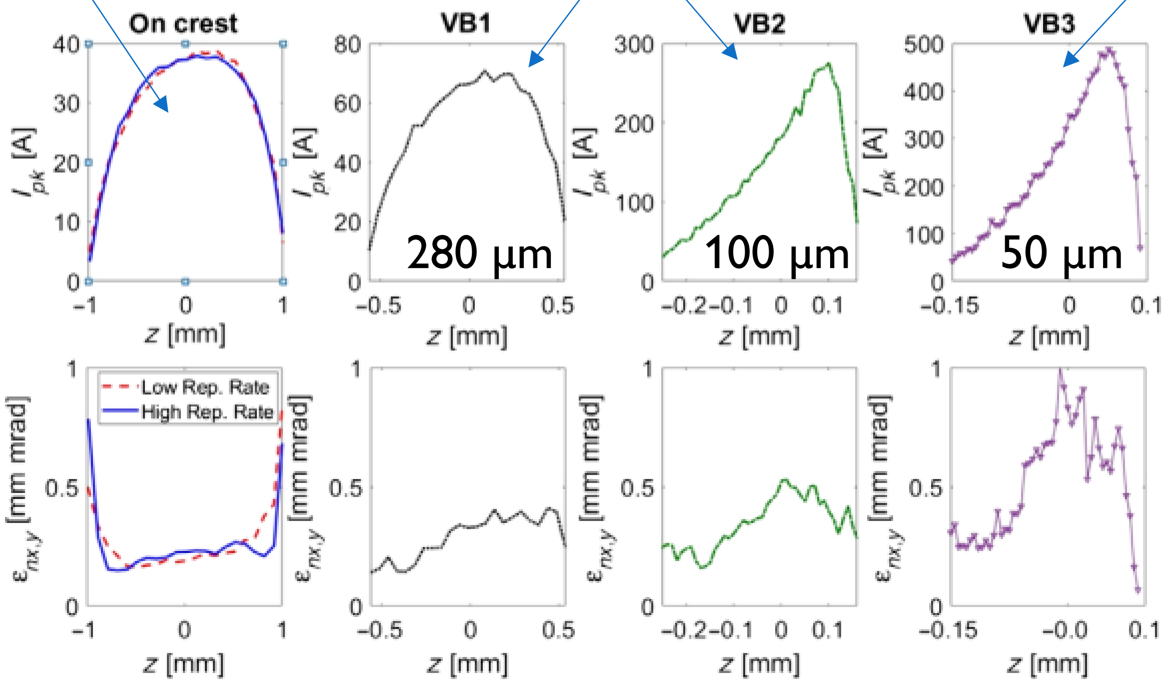

FIG. 5. Slice analyses of the transverse normalized emittance and of the peak current for different compression factors in case of velocity bunching operation. The VB 1 to 3 are related to the case of final beam length of 280, 100, and 50 µm, respectively.

The 2.6 cell C-band gun [6]

- The gun is a 2.6-cell standing wave (SW) structure operating with a peak field (E_{cath}) at the cathode of 160 - 180 MV/m.
- A four-port mode launcher with an on-axis coupling has been adopted to reduce the pulsed heating on the coupler and to perfectly compensate the dipole and quadrupole field components
- The insertion of the mode launcher has opened to an increased flexibility in positioning the input waveguide relative to the gun body that results in a more powerful cooling capability of the accelerating cells especially useful in the high repetition rate operation (1 kHz)

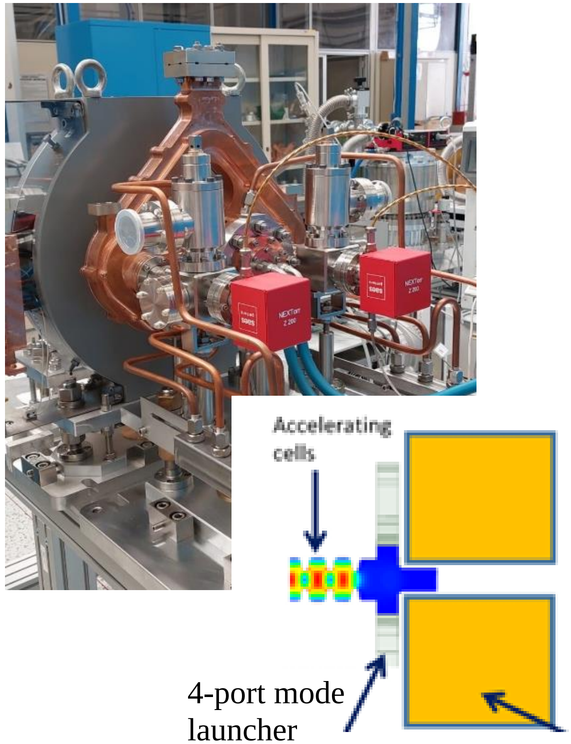

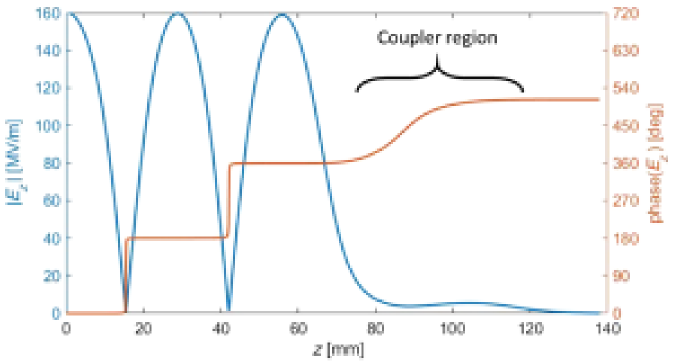

FIG. 7. Amplitude and phase of the longitudinal electric field along the beam propagation axis. The plot also includes the mode launcher region, where the field presents a traveling wave component (nonconstant phase) related to the power flow into the gun.

TABLE II. Main gun parameters for the 100 Hz operation rate and for the 400 Hz repetition rate (in parenthesis), the latter being the maximum operation rate for available commercial klystrons [43].

Working frequency (GHz)	5.712
$E_{cath}/P_{diss}^{1/2}$ [MV/(mMW$^{1/2}$)]	51.4
rf input power (MW)	23 (18)
Cathode peak field (MV/m)	180 (160)
Cathode type	copper
Rep. rate (Hz)	100 (400)
Quality factor	11900
Filling time (ns)	166
Coupling coefficient	3
rf pulse length (ns)	300
E_{surf}/E_{cath}	0.96
Modified Poynting vector (W/μm^2)	3.2 (2.5)
Pulsed heating (°C)	20 (16)
Average diss. Power (W)	320 (1000)

[6] D. Alesini et al., Design, realization and high power RF test of the new brazed free C band photo-gun, Proc. IPAC'24, 2024

TW accelerating structures

- The C-band traveling wave module is made up of four 2 m long traveling wave accelerating structures fed by one klystron and one pulse compressor

ELI-NP dumped cells for **multi-bunch operation** (100 Hz)

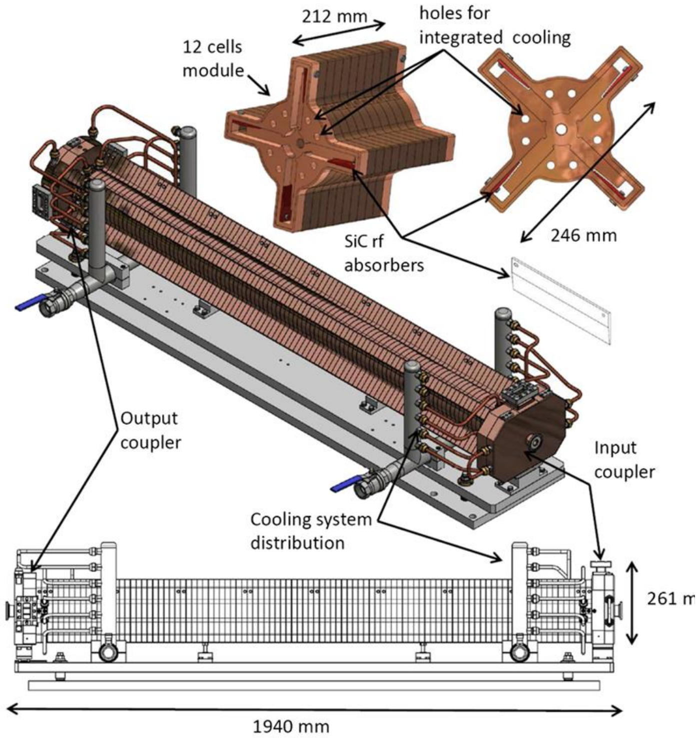

TABLE I. Main parameters of the ELI-NP accelerating structures.

Parameter	Value
Working frequency (f_{rf})	5.712 GHz
Cell phase advance	$2\pi/3$
Number of cells	102
Structure length	1.8 m
Iris aperture radius	6.8–5.78 mm
Repetition rate	100 Hz
Average quality factor	8850
Average accelerating field	33 MV/m
Shunt impedance	67–74 MΩ/m
Group velocity (v_g/c)	0.025–0.015
Filling time	313 ns
rf input power (P_{in})	40 MW
Output power (P_{out})	$0.29P_{in}$
Pulse duration for beam (τ_{beam})	<512 ns
Pulsed heating (input coupler)	<21 °C
Average wall-loss power	2.3 kW
Working temperature	30 °C

D. Alesini *et al*,0.1103/PhysRevAccelBeams.23.042001

Compact Light TW cells for high rep rate (100 -400 Hz)

TABLE IV. Main parameters of the *C*-band structures (in parenthesis we have reported the 400 Hz repetition rate case).

Working frequency (GHz)	5.712
Phase advance per cell (rad)	$2\pi/3$
Average iris radius $\langle a \rangle$ (mm)	6.6
Iris radius **a** (mm)	6.94-6.26
Number of cells per structure	120
Accelerating cell length (mm)	16.67
Structure length $\mathbf{L}_s$ (m)	2
Shunt impedance **R** (MΩ/m)	71–77
Effective shunt impedance $\mathbf{R}_s$ (MΩ/m)	190
Group velocity v_g/c (%)	2.4–1.6
Filling time (ns)	336
Average acceleration gradient (MV/m)	31 (15)
Required input power per module (MW)	41 (9)
Number of structure in the module	4

Courtesy of A. Vannozzi et al.

- Axial symmetric 2D simulations have been performed with Poisson Superfish
- Solenoids specifications in terms of focal length and peak field are defined by the WP definition → Invariant Envelope with and without RF compression [7.8.9]

Gun solenoid

The gun solenoid is a 12 cm long device consisting in a single coil with bore radius of 3 cm

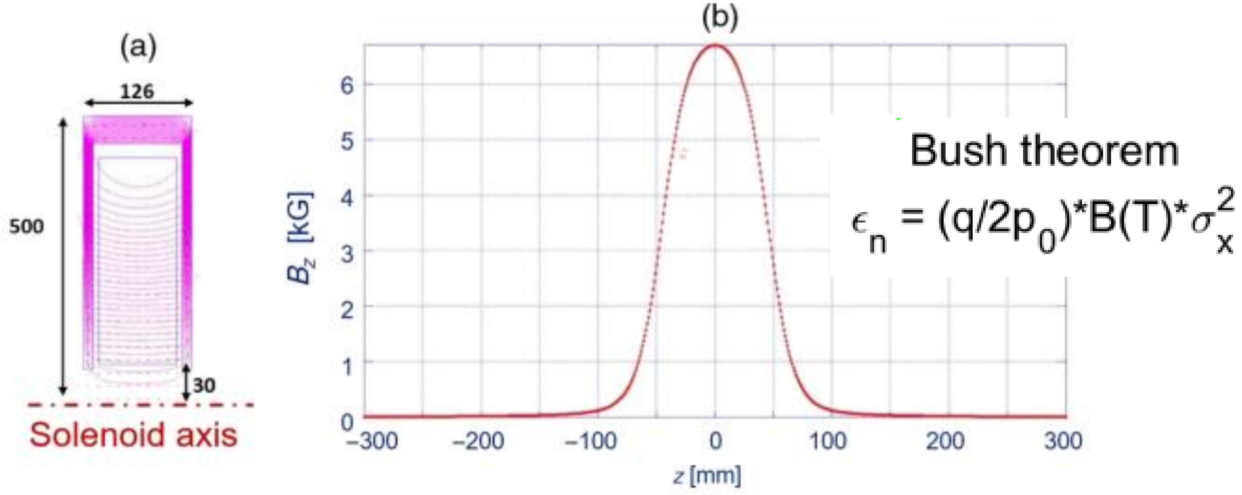

Bush theorem

$$\epsilon_n = (q/2p_0)*B(T)*\sigma_x^2$$

FIG. 9. (a) Solenoid geometry (dimensions are in mm) and (b) the on-axis magnetic field as obtained by means of Poisson-Superfish simulations.

TW acc. Solenoid

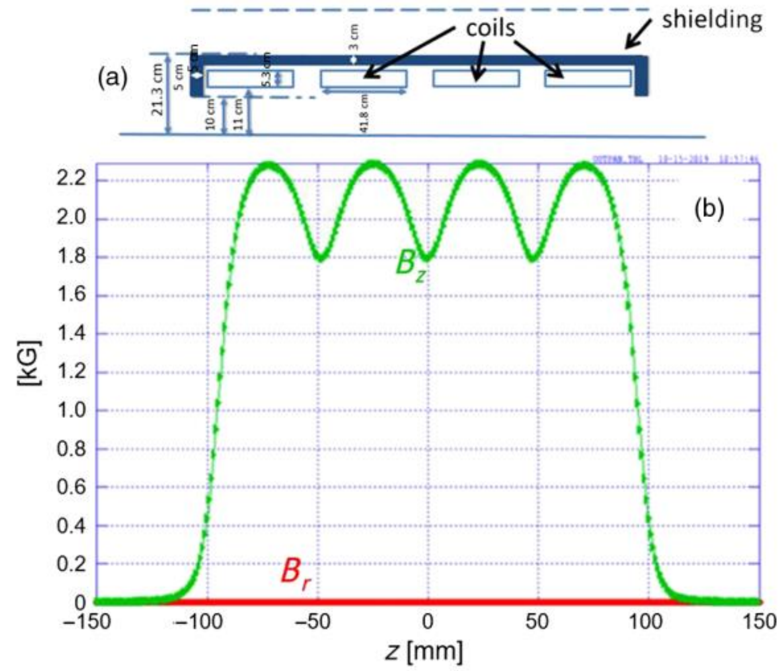

FIG. 11. (a) Geometry of the C-band solenoid simulated with Poisson-Superfish (dimensions are in mm); (b) longitudinal (B_z) and radial (B_r) magnetic field on axis.

[7] B. E. Carlsten, NIM A 285, 311-319 (1989)
[8] L. Serafini, J. B. Rosenzweig, Phys. Rev. E 55, 75657590 (1997)
[9] L. Serafini and M. Ferrario, ‘Velocity bunching in photoinjectors’ AIP Conf. Proc., vol. 581, no. 1, pp. 87–106, 2001. doi:10.1063/1.1401564

EuPRAXIA@SPARC_LAB – the C-band proposal

- **EuPRAXIA@SPARC_LAB** aims to a build the first ever plasma-based FEL user facility within the **PWFA** technique
- The main working point foresees an FEL emission at 4 nm with flux of ≈10^{12} ph/pulse
- The PWFA scheme relies on train of femto-second long bunches for FEL radiation
    - 200-400 pC driver and 30-50 pC witness separated by less than 1 ps
    - Generated through the RF compression

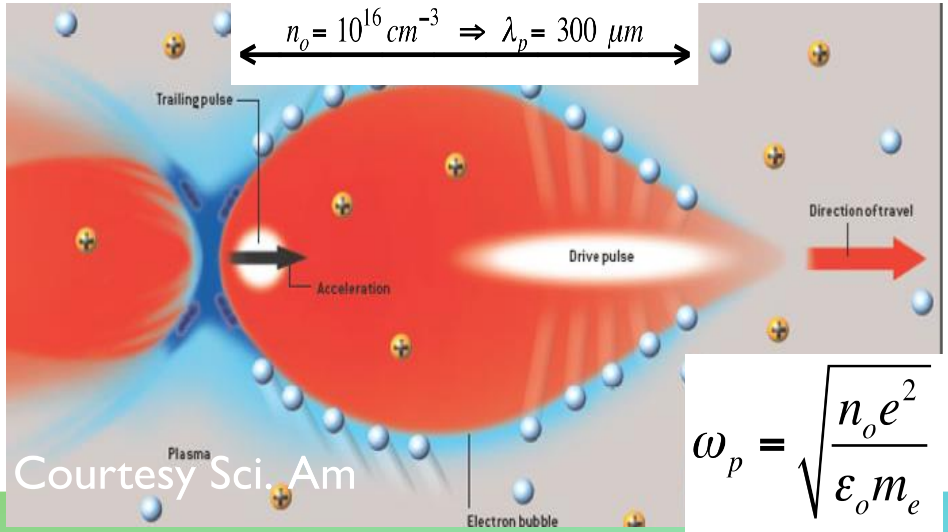

$n_o = 10^{16}\ cm^{-3} \Rightarrow \lambda_p = 300\ \mu m$

$$\omega_p = \sqrt{\frac{n_o e^2}{\varepsilon_o m_e}}$$

Courtesy of G.J. Silvi et al.

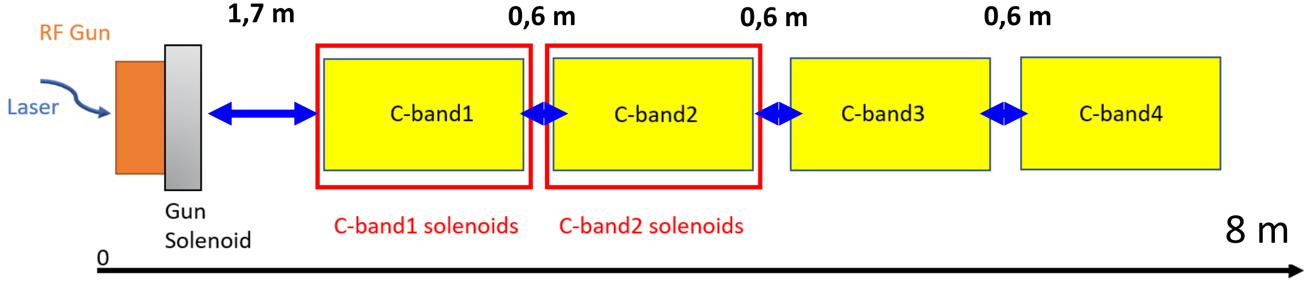

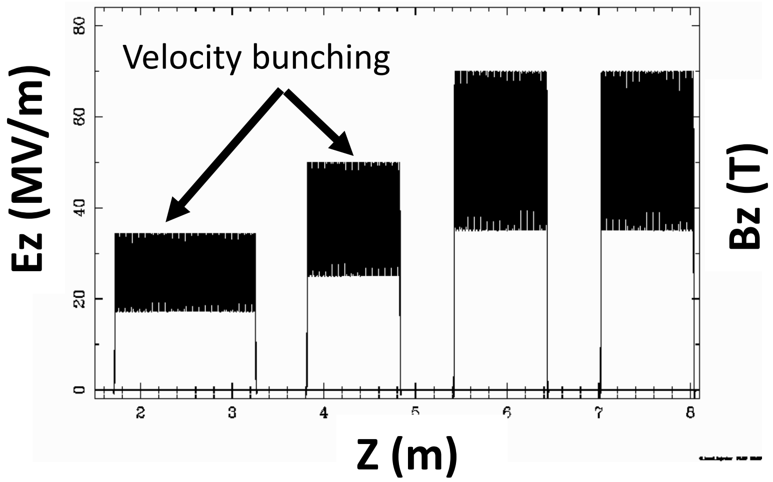

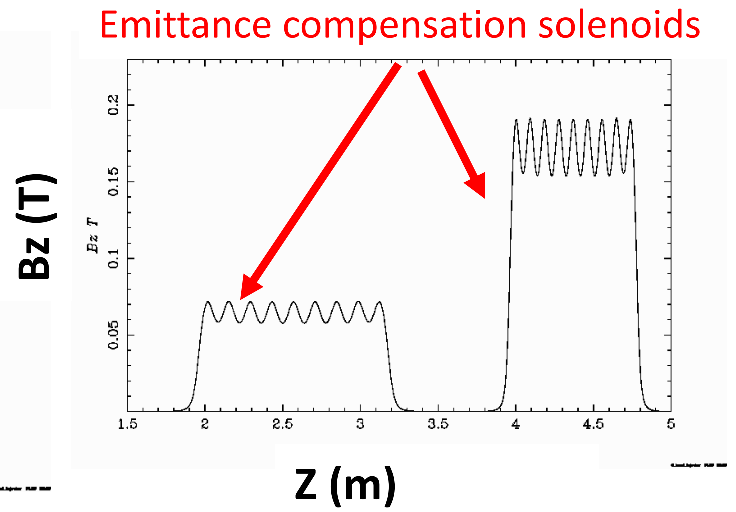

[10] G.J. Silvi et al. "Beam dynamics optimization of EuPRAXIA@SPARC_LAB RF injector" J.Phys.Conf.Ser. 2687 (2024) 6, 06202

Beam dynamics simulations

Funded by the European Union

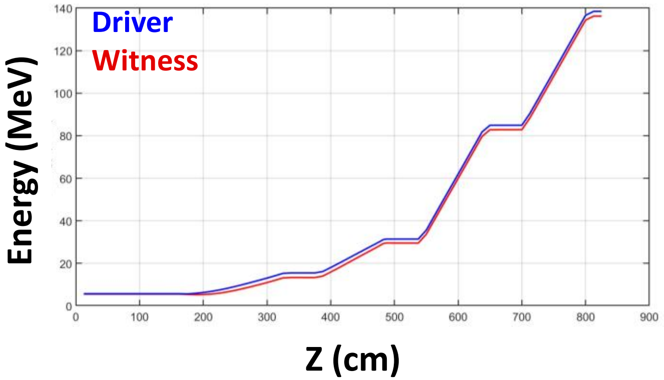

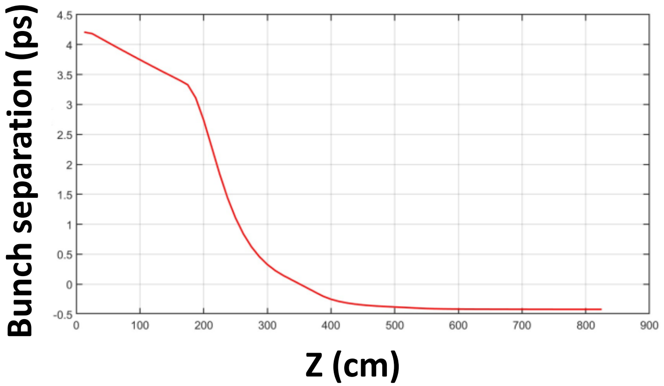

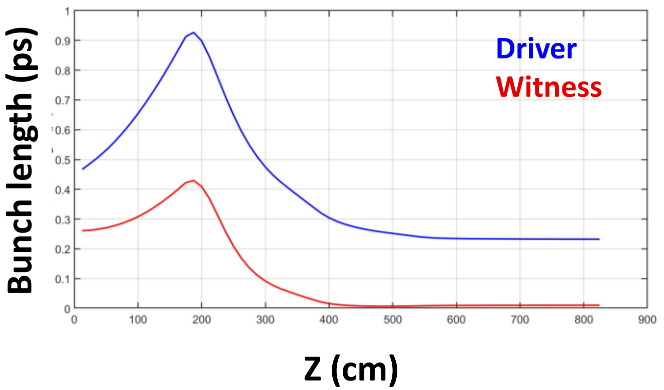

Witness	Driver
30 pC	200 pC
0,2 mm rms	0,32 mm rms
100 fs	100 fs
	11,5 ps (driver delay)

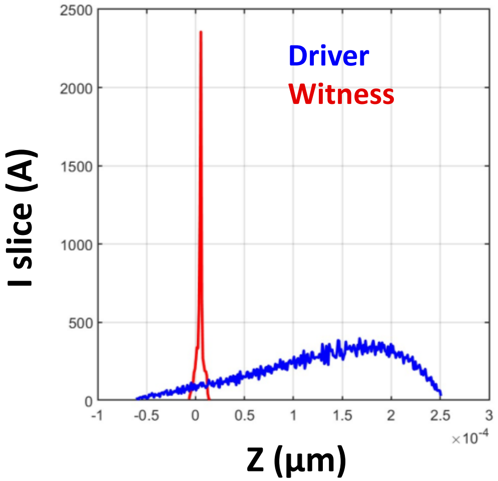

Injector exit parameters	Witness / Driver
Emittance (mm-mrad)	0,6 / 2
Energy (MeV)	136 / 138
Energy spread (KeV)	3,5 / 5,8
Bunch separation (ps)	0,45
Bunch length (um)	3,2 / 70

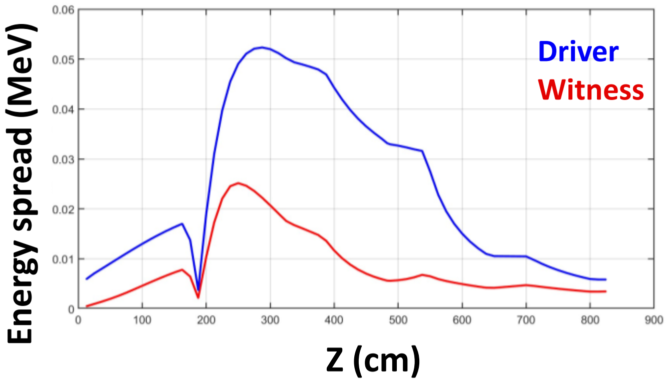

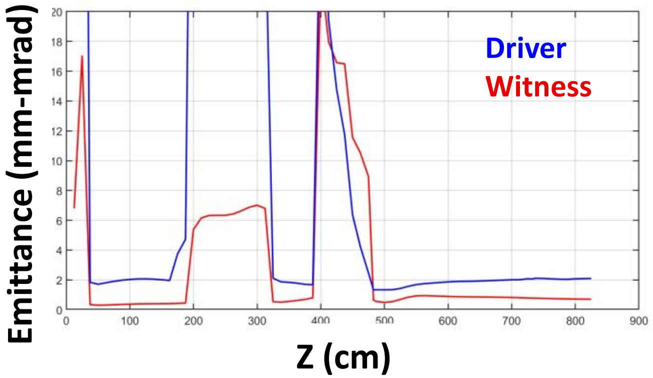

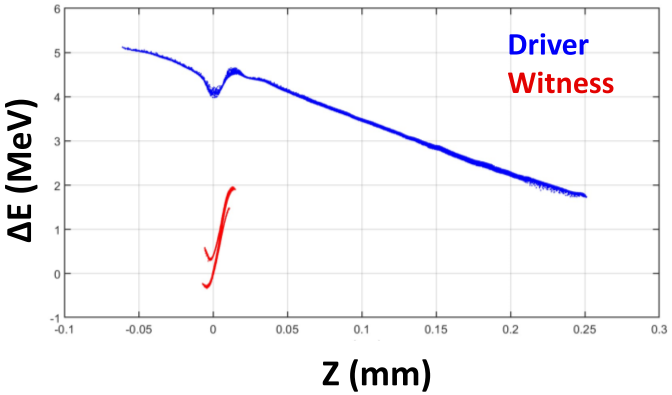

[11] A. Giribono et al. EuPRAXIA@SPARC_LAB: The high-brightness RF photo-injector layout proposal, NIMA (2018)

Stability improvement with a Ka-band linearizer

Funded by the European Union

SW Ka-band	
Resonant Frequency	36 GHz
E acc	10 MV/m
Number of cells	19
Length	8 cm
Radius	3,5 mm

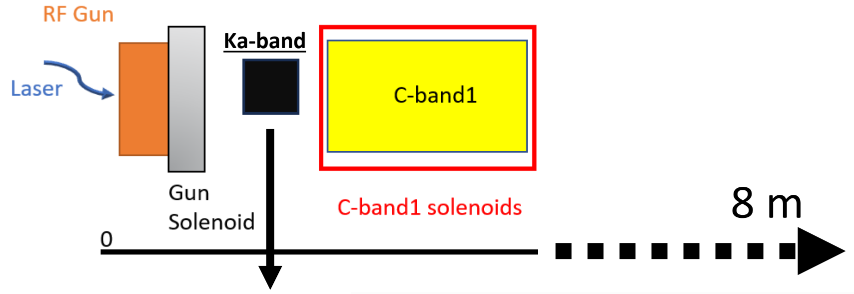

Injector exit parameters	Witness / Driver
Emittance (mm-mrad)	0,48 / 2,46
Energy (MeV)	136 / 138
Energy spread (KeV)	4,6 / 4,8
Bunch separation (ps)	0,5
Bunch length (um)	3,7 / 56

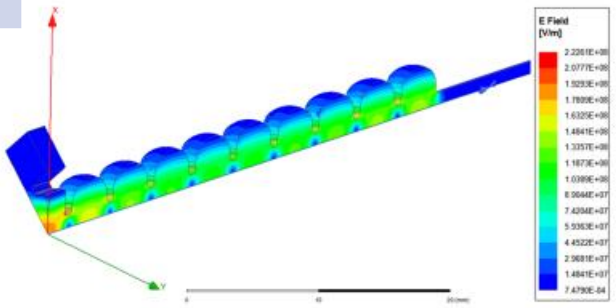

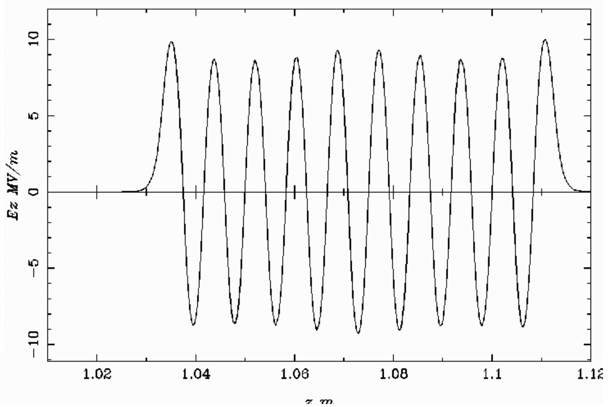

[12] M. Behtouei et al. 'A SW Ka-Band linearizer structure with minimum surface electric field for the compact light XLS project, NIMA vol 894 (2020) https://doi.org/10.1016/j.nima.2020.164653

Driver

Witness

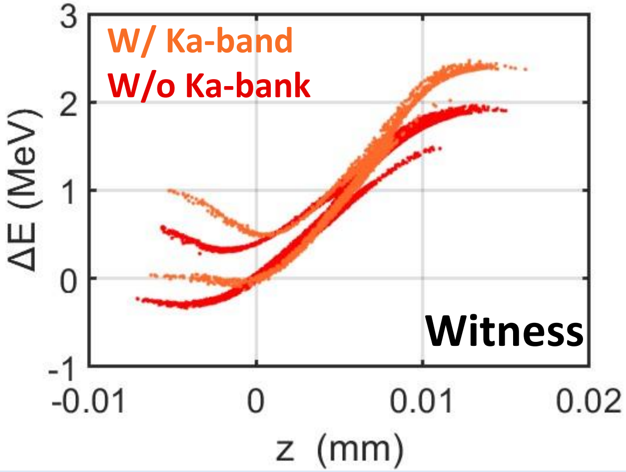

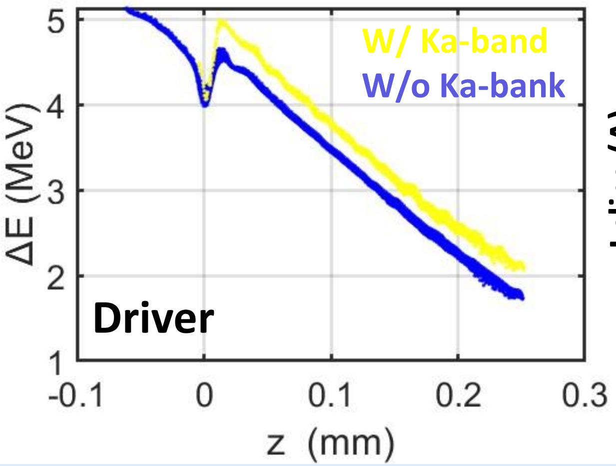

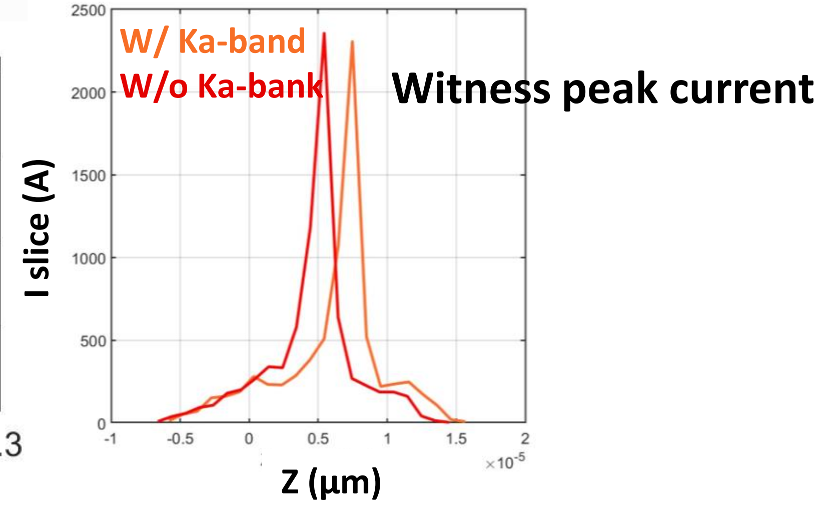

EuRIZON – C-band linac for FEL emission

parameter	value
energy	6 GeV
espread	2 MeV
peak current	5 kA
emittance, norm.	0.6 mm mrad
rms bunch length	6μm -> 20fs (250pC)

- One of the Eurizon project goal is the definition of a 6 GeV injector useful for high brightness soft Free Electron Laser with emission of radiation at 4 nm and high brilliance

- Beam dynamics simulations have been performed for a 250 pC electron beam from the cathode up to the FEL entrance

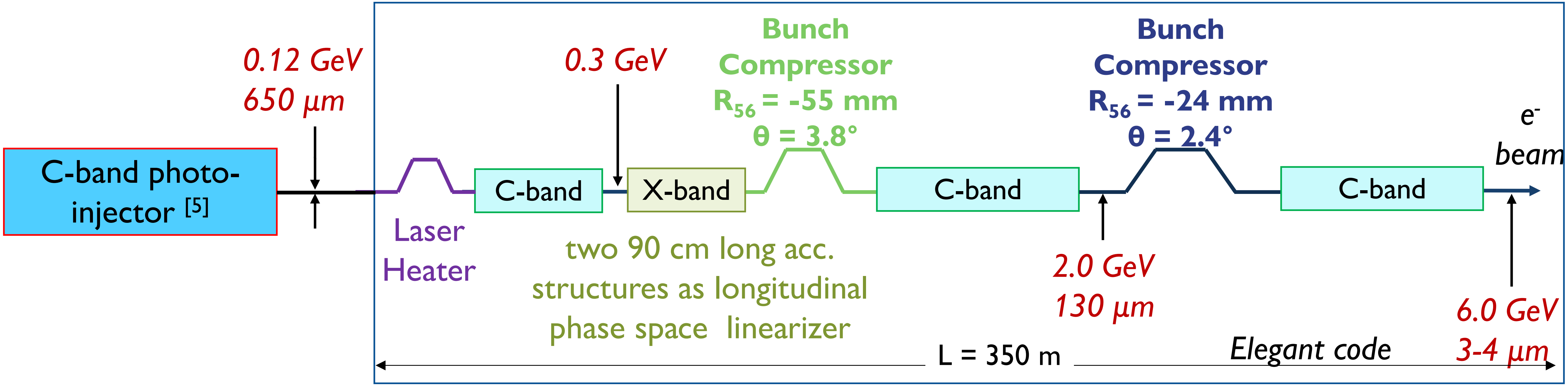

The booster linac design started from the Swiss FEL CDR [12,13]

[13] https://www.psi.ch/sites/default/files/import/swissfel_old/CurrentSwissFELPublicationsEN/SwissFEL_CDR_V20_23.04.12_small.pdf
[14] Eurizon Milestone D4.20 and D4.19 - https://www.eurizon-project.eu/

Beam Dynamics Studies – Eurizon WP

- **The beam dynamics has been studied by means of simulations with the *ASTRA* code**
- A 250 pC beam is used as reference working point
  - The beam distribution at the cathode has been chosen looking at the beam quality at the photoinjector exit
    - Flat-top 8.5 ps fwhm
    - Transverse uniform profile with 170 μm rms beam size
  - The photoinjector is sets **on-crest** to obtain as much as possible low transverse emittance @ph.exit in accordance with the invariant envelope condition [7.8]

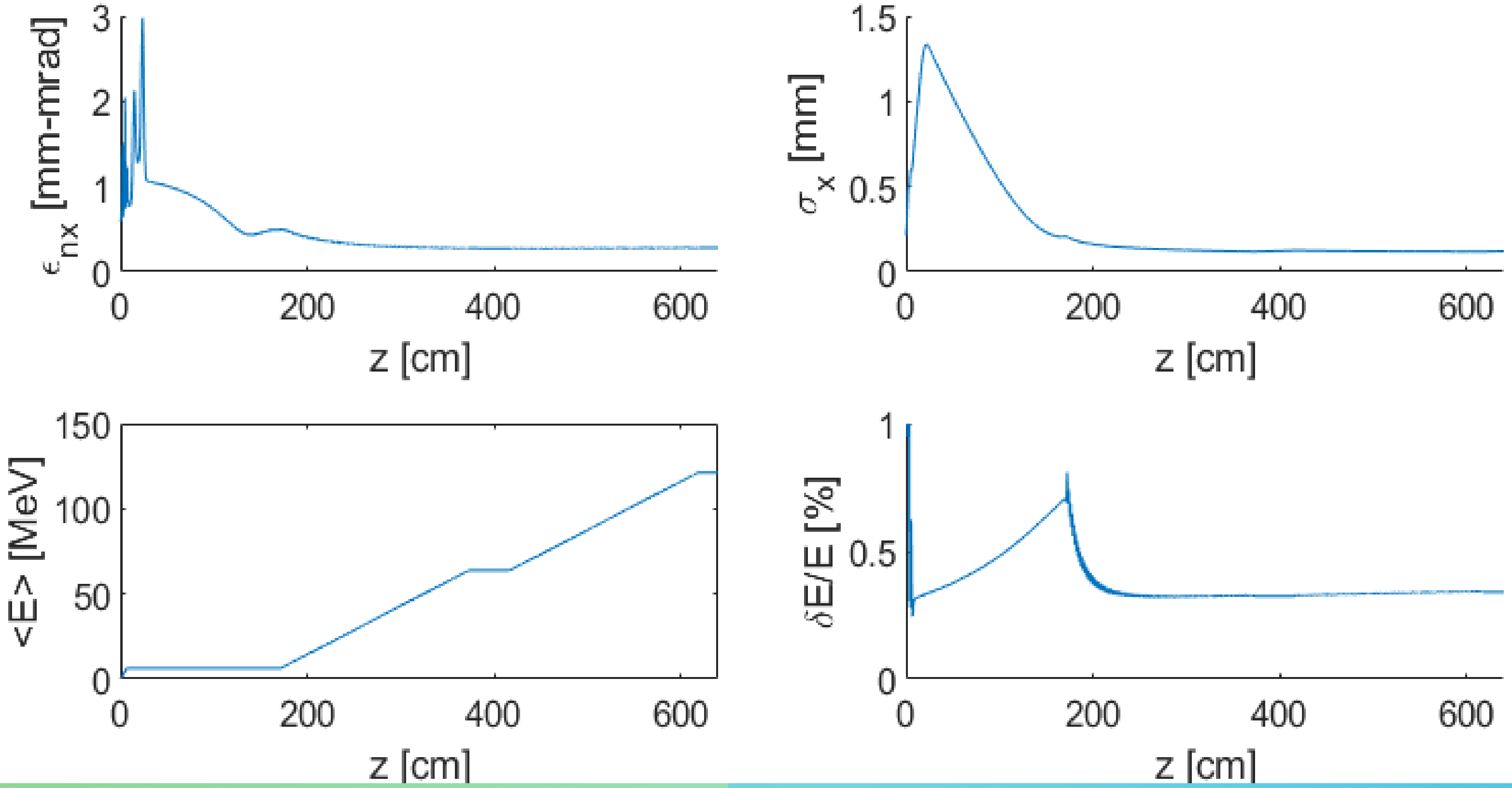

Parameters @ph. exit	Sim. results	units
Q	250	pC
E	122	MeV
σ_E/E	0.34	%
$\epsilon_{n,rms}$	0.28	μm
σ_z	670	μm
I_{peak}	35	A

EuRIZON – the transverse phase space in the linac

Twiss function along the C-band booster linac

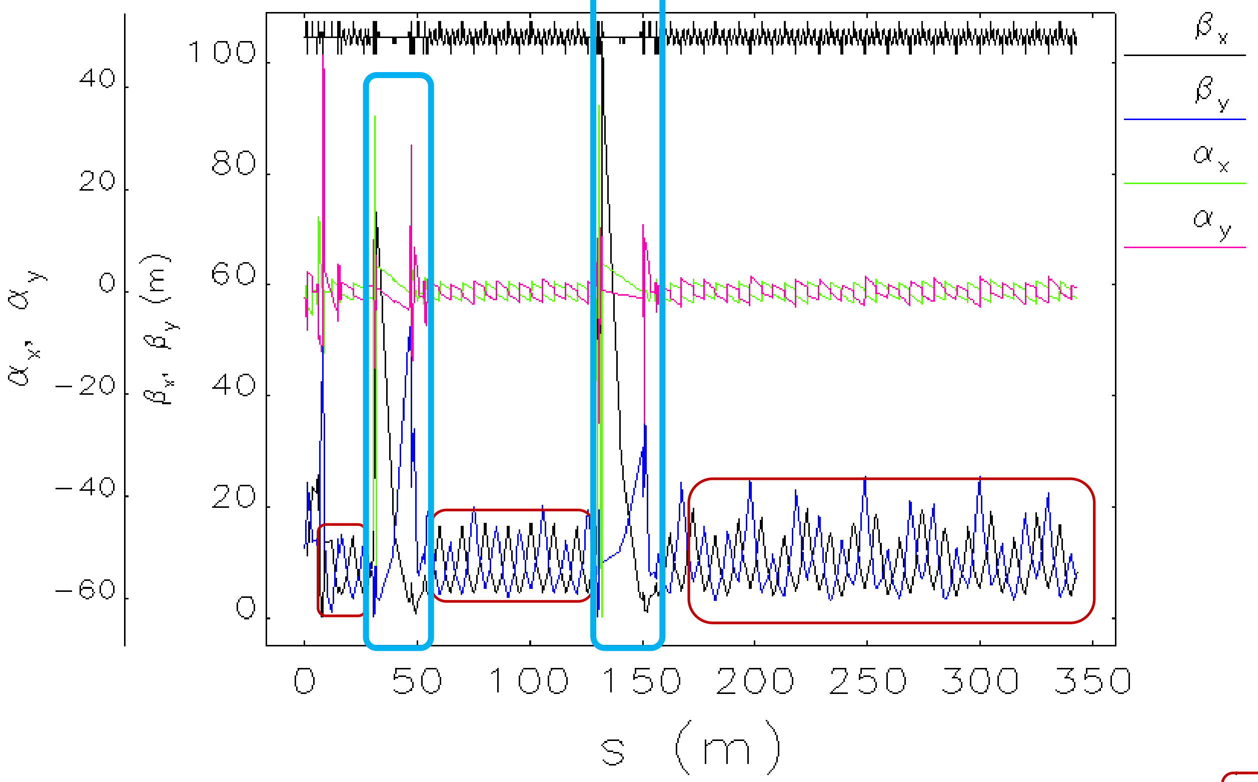

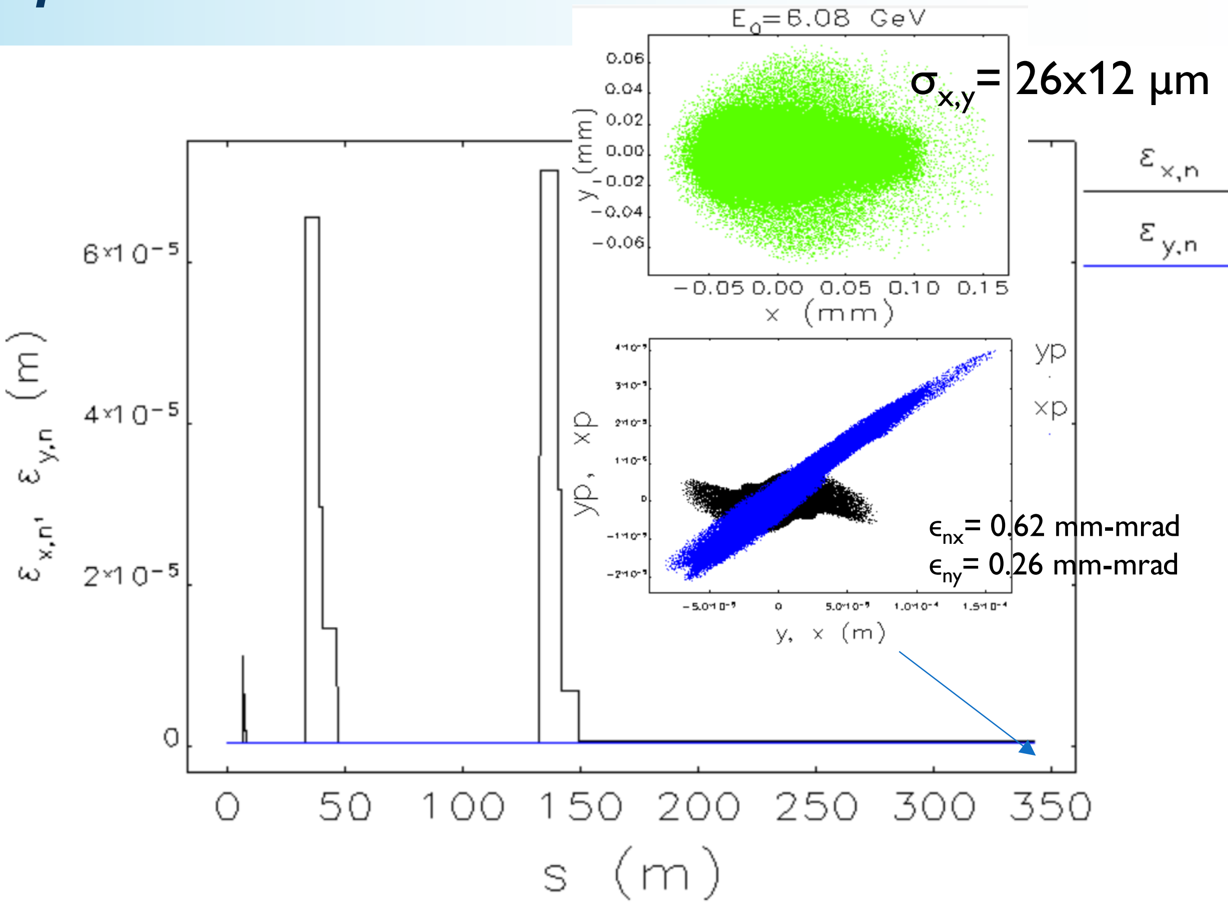

simple matching has been adopted to proper match the beam at

the Linac section entrance to transport it through the linac (FODO like)

the LH, BC1 and BC2 entrance (no emittance dilution)

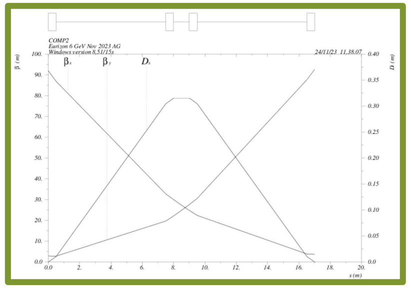

EuRIZON – the longitudinal phase space and the micro-bunching

- The beam is boosted in energy and longitudinally compressed to obtain a 5kA peak current, less than 0.6 mm-mrad slice emittance and less than 2 MeV slice energy spread (<0.04%)

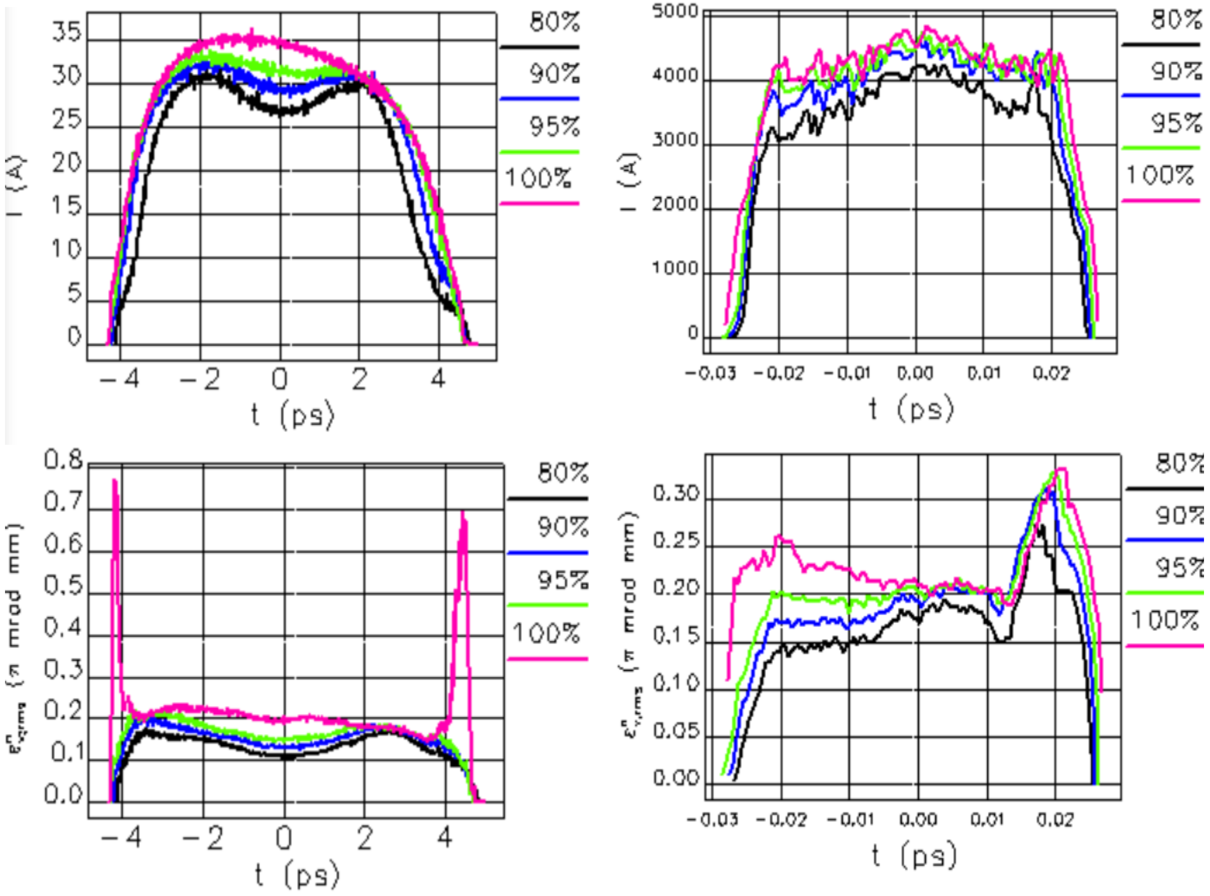

Slice analyses at the photoinjector (left) and booster linac (right LH on) exit

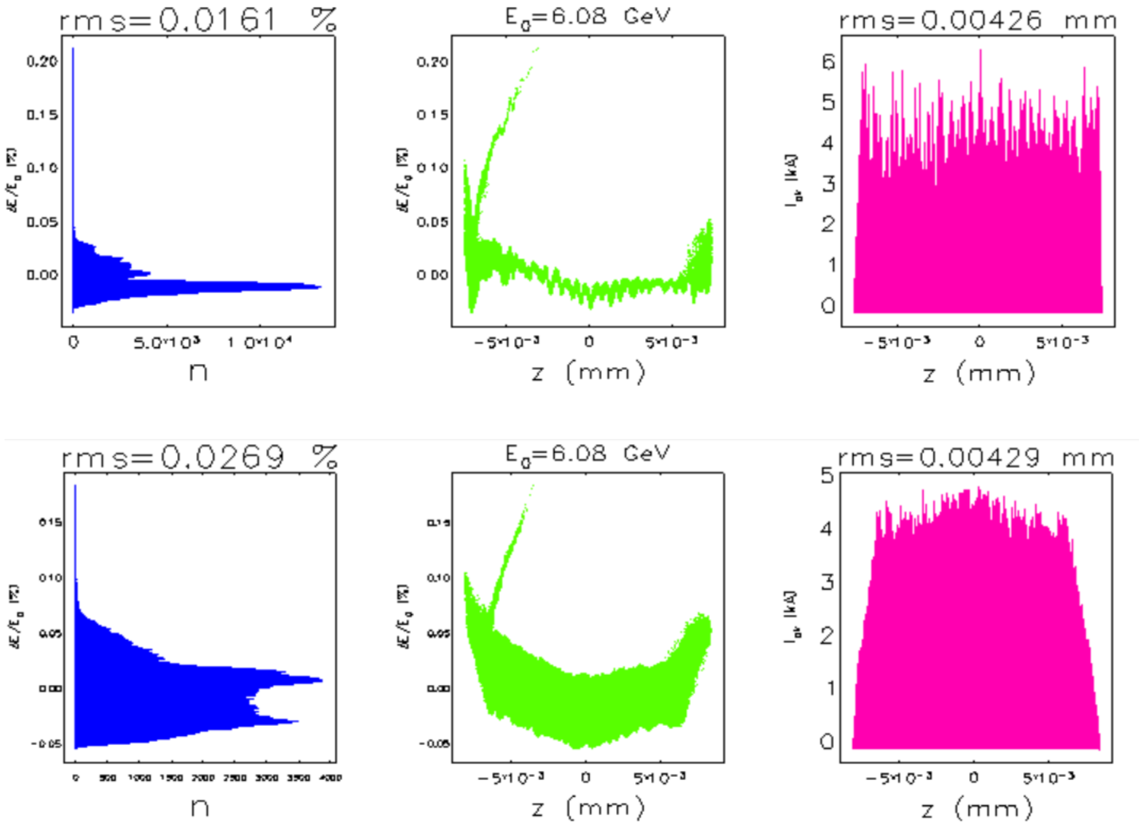

LPS analyses at 6 GeV with the laser heater switched off (up) and on (down)

The BoCXS proposal

Bologna Compton X-ray Source ⟶ ICS-based light source

Courtesy of G. Campri

Massimo Placidi, Guest Lawrence Berkeley National Laboratory;
massimoplacidi@icloud.com

Giovanni Campri, Sapienza University of Rome;
giovanni.campri@uniroma1.it

Anna Giribono, **David Alesini**, INFN-LNF;
Anna.Giribono@lnf.infn.it (A.G.); david.alesini@lnf.infn.it (D.A.)

Simone Di Mitri, Elettra-Sincrotrone Trieste;
simone.dimitri@elettra.eu

Armando Bazzani, **Giorgio Turchetti**, University of Bologna;
armando.bazzani@unibo.it (A.B.); giorgio.turchetti@unibo.it (G.T.)

High quality X-ray beam

- Tunable energy (50-700 keV)
- Quasi-monochromatic
- Short pulses (ps)
- Reasonably high fluxes ($\sim 10^{10}$ ph/s)

Multidisciplinary applications

- Biomedical imaging
- Industrial applications
- Cultural heritage science
- …and more!

Linearization with the X-band cavity

The need for linearization

The chromatic aberrations in the quadrupoles had a large impact on the beam emittance.

A significant current profile modulation inside the doglegs, due to the coupling of R_{56} with the energy chirp, caused beam quality degradation through Coherent Synchrotron Radiation (CSR) effects.

The cause was a strong quadratic energy chirp, due to the curvature of the RF fields inside the C-band photo-injector.

All these effects caused emittance growth of up to 100%, and made it very difficult to optimise the magnetic lattice.

This project has received funding from the European Union's Horizon
programme under GA No101004730

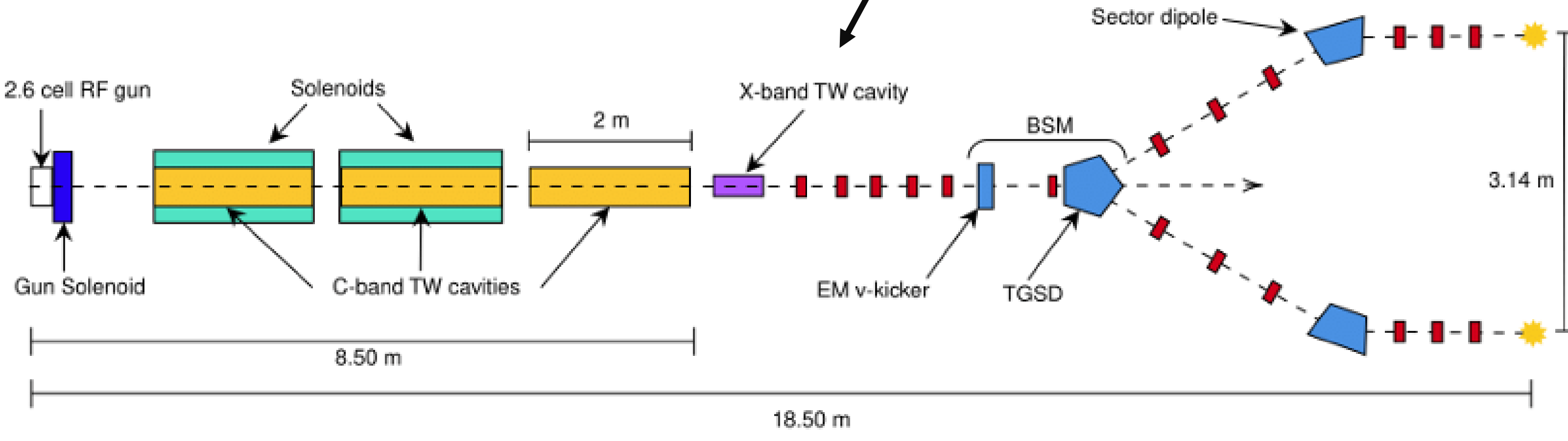

Fig. 2 – BoCXS schematic machine layout (not to scale). These are all the elements included in the beam simulations.

[15] A. Bazzani et al. 'BoCXS: A compact multidisciplinary X-ray source' Physics Open Volume 5, 100036 (2020) https://doi.org/10.1016/j.physo.2020.100036

BoCXS: beam dynamics studies

The RF photoinjector

Simulated with ASTRA (500k particles)

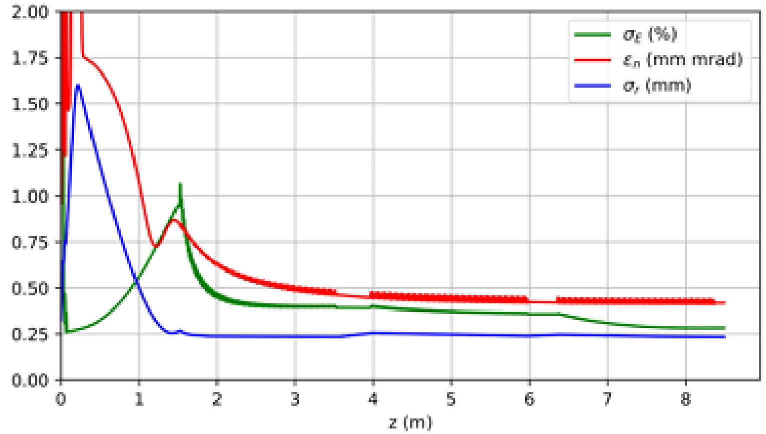

The transfer line

Fig. 18 – Beam dynamics simulation along the the beamline.

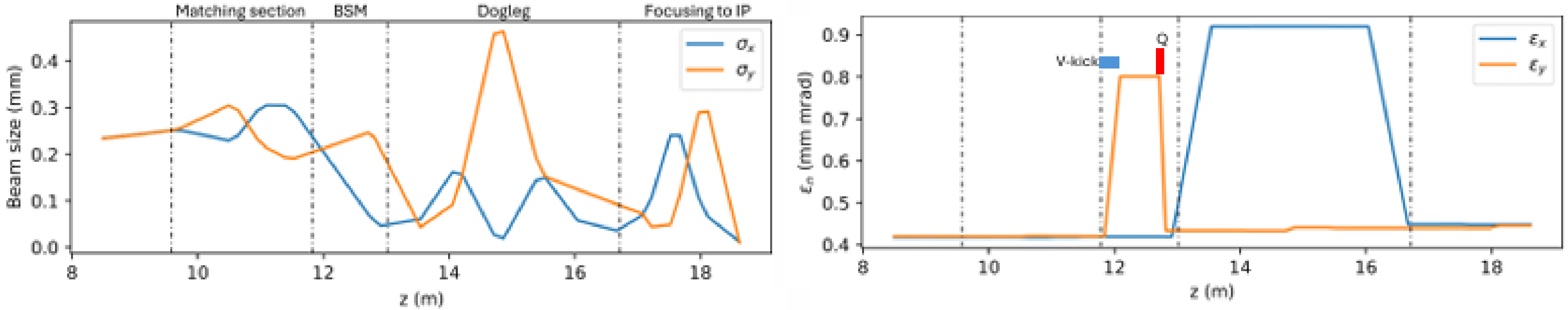

@IP

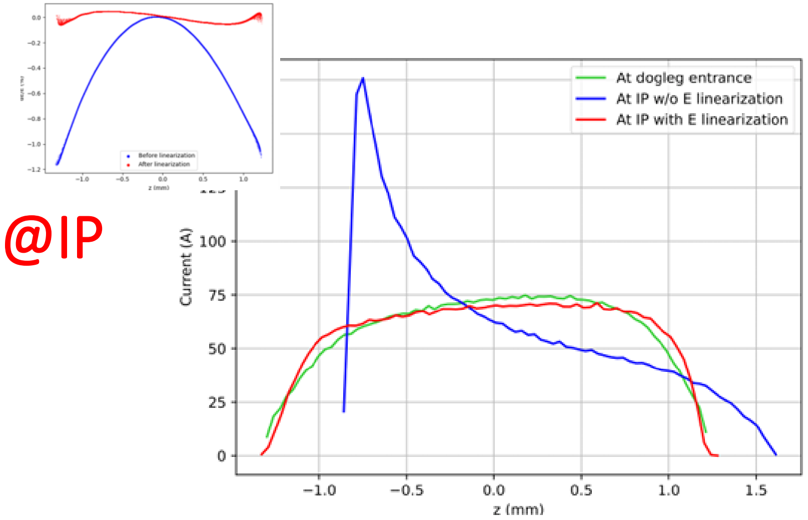

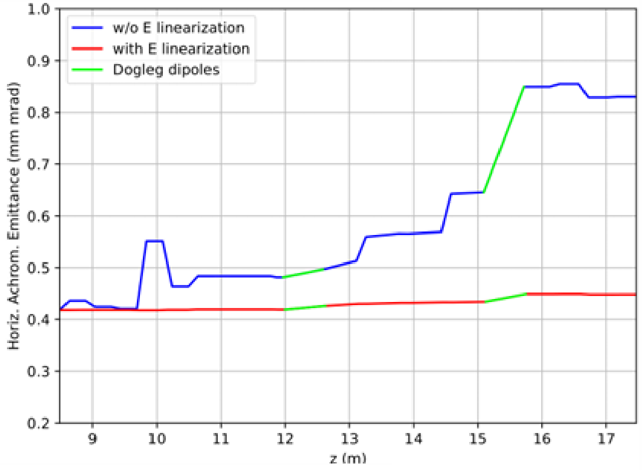

Tab. 6 – Electron beam parameters at IP

Parameter	Value
Bunch charge [nC]	0.5
Beam energy [MeV]	145
Norm. proj. emittance [mm mrad]	0.45
Bunch length, rms [ps]	2.2
Horizontal beam size, rms [μm]	12.0
Vertical beam size, rms [μm]	10.0
Relative energy spread, rms [%]	0.03
Peak current [A]	71

BoCXS ICS X-ray source

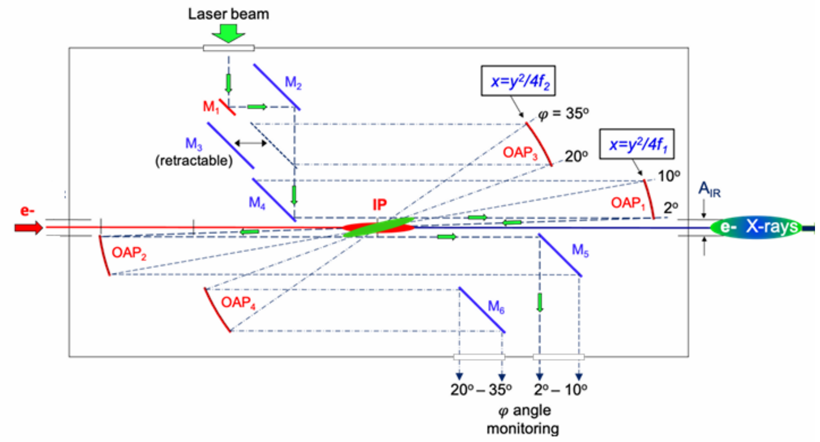

Fig. 24 – Layout of the optical box at one of the BoCXS laser-electron interaction regions. Two sets of OAP mirrors select the interaction angle φ within an operational range $\Delta\varphi_1 = 2^o - 10^o$ (M_4 – OAP_1) and a larger set $\Delta\varphi_2 = 20^o - 35^o$ (M_3 – OAP_3) to produce X-ray energy shifts of the order of 2–3 keV for KES dual-energy imaging. The angle φ is defined by the position of the scanning mirror M_1 and monitored through the $M_{5,6}$ extracting mirrors.

Tab. 7 – Laser parameters at IP

Parameter	Value
Rep. rate [kHz]	0.1
Central wavelength [nm]	1032-516
Bandwidth, FWHM [%]	1
Beam quality factor	<1.5
Pulse energy [J]	1.0
Intensity pulse size, rms [µm]	10.0
Pulse duration, rms [ps]	3.0

X-rays expected parameters

Tab. 8 – Compton X-ray expected parameters for an interaction angle of 2 deg

Parameter	1° laser harmonic	2° laser harmonic
Rep. rate [kHz]	0.1	
Pulse duration, rms [ps]	2.7	
Source size, rms [µm]	5.1	
Source divergence, rms [mrad]	2.7	
Max. photon energy [keV]	384.5	769.0
Total peak intensity [ph/pulse]	$3.7 \cdot 10^8$	$1.9 \cdot 10^8$
Total peak power [W]	$2.8 \cdot 10^6$	
Total average intensity [ph/s]	$3.7 \cdot 10^{10}$	$1.9 \cdot 10^{10}$
Total average power [W]	$7.6 \cdot 10^{-4}$	
Peak brilliance [ph/s/mm²/mrad²/0.1%BW]	$1.0 \cdot 10^{19}$	$5.0 \cdot 10^{18}$
Average brilliance [ph/s/mm²/mrad²/0.1%BW]	$6.8 \cdot 10^9$	$3.4 \cdot 10^9$
Average spectral density [ph/s/0.1%BW]	$5.6 \cdot 10^7$	$2.8 \cdot 10^7$

Fig. 25 – ICS intensity vs. photon energy (blue) and average photon energy vs. observation angle (red).

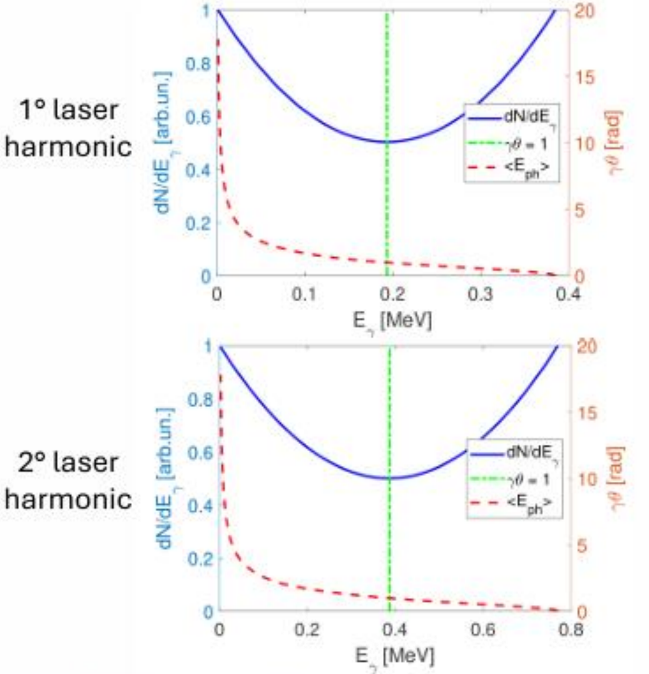

18

Summary

- The design of a normal conducting – high repetition rate full C-band photoinjectors has been shown
- It is suitable for driving several applications as
  - Plasma or higher harmonic accelerating cavities
  - Radiation sources
  - Other applications which require for high flux and/or high quality electron beams

- In the next future:
  - Further studies will be performed in the next future to evaluate longitudinal instabilities that could arise mainly related to RF compression which can provide hundreds of fs long beams for relative high charge (nC range) and the machine sensitivity (already addressed for the EuPRAXIA case)
  - The C-band gun is under testing at PSI and will be mounted at the TEX facility at INFN-LNF
    - EuPRAXIA
    - Medical applications (LATINO)
- Special acknowledgment to D. Alesini, G. Campri, S. Di Mitri, G. J. Silvi, C. Vaccarezza, the BoCXs, EuRIZON, XLS, IFAST and EuPRAXIA collaborations for materials and fruitful discussions

THANK YOU FOR YOUR ATTENTION

BACKUP SLIDES

RF-PHOTOINJECTORS

TRANSVERSE BEAM EMITTANCE

- In the photoinjector the electron beam is emitted from the cathode surface, illuminated by a laser pulse, when the applied RF accelerating field overcomes the electric field produced by the electron bunch itself—image and space charge fields.
- The properties of the photoelectrons arising from the cathode determine the beam intrinsic emittance that represents the ***lowest beam emittance value one can expect at the photoinjector exit***

$$\epsilon_{intrinsic} = \sigma_x \sqrt{\left(\frac{m^*}{m}\right)\left(\frac{\hbar\omega - \phi_{eff}}{3mc^2}\right)}$$

full width of the emitted electron energy spectrum

$$\phi_{eff} = \phi_w - \phi_{Schottky} = \phi_w - \alpha\sqrt{\beta E_{RF}} = \phi_w - e\sqrt{\frac{e}{4\pi\varepsilon_0}(\beta E_{RF})}$$

Courtesy of J. Scifo Athens XLS meeting

Cathode material	E_{RF}^{peak}[MV/m]	σ_{rms} [mm]	$\varepsilon_{n,int}$ [μm]	QE
Cu	240	0.17	0.12	10^{-5}-10^{-4}

- Once emitted, the electrons beam experiences external and internal forces that degrade the beam quality as
  - strong self-fields → space charge emittance oscillations
  - fields in the accelerating cavities → emittance oscillations
  - fields of the transport optics → chromatic and geometric aberrations

$$\varepsilon = \sqrt{\varepsilon_{int}^2 + \varepsilon_{roughness}^2 + \varepsilon_{rf}^2 + \varepsilon_{SC}^2 + \varepsilon_{solenoid}^2}.$$

BEAM EMITTANCE COMPENSATION

- It is possible to restore the initial transverse emittance value by
  - properly setting the magnetic field of the solenoid surrounding the gun to counteract the beam internal space charge forces and the external rf kick
  - pushing quickly the beam up to relativistic energy to freeze the beam transverse emittance
  - Applying the **invariant envelope** theory: if a downstream booster section follows the gun, it is recommended to place it where the beam emittance exhibits its maximum and to set the gun solenoid so to let the emittance oscillations damp down to the intrinsic value; that way the beam is quickly pushed up to relativistic energy and the emittance oscillation can be frozen and its minimum at the exit of the accelerating section
- The laser pulse setup determines the emittance quality
  - **pancake beams** → very short beams, higher transverse emittance
  - **cigar beams** → pulse length in the mm range so to reduce the emittance degradation due to the transverse space charge forces before the beam becomes ultrarelativistic. This set point allows for an electron beam with sub mm mrad transverse emittance

$$F_x = \frac{e\hat{I}x}{8\pi\gamma^2\varepsilon_0\sigma_x^2\beta c} g(\zeta)$$

Space charge defocusing is primarily a non-relativistic effect and decreases as γ^{-2}

Envelope equation:

$$\sigma'' + \frac{\gamma'}{\gamma}\sigma' + \left(\frac{k}{\gamma}\right)^2 \sigma = \frac{I}{2I_A\gamma^3\sigma} + \frac{\varepsilon_n^2}{\gamma^2\sigma^3}$$

Invariant envelope criteria:

- laminar envelope waist ($\sigma' = 0$)
- σ matched to the accelerating and focusing gradients to stay close to an equilibrium mode

$$\sigma = \frac{1}{k}\sqrt{\frac{I_0}{4\gamma_0 I_A}\left(1 + \sqrt{1 + \left(4\frac{\varepsilon_n\gamma_0 k I_A}{I_0}\right)^2}\right)}$$

EuPRAXIA@SPARC_LAB

- EuPRAXIA@SPARC_LAB is a multi-GeV plasma-based accelerator with outstanding beam quality to drive a user facility whose main application concerns the operation of a soft X-ray FEL (3-5 nm)
- The **'WP1-Accelerator Physics'** focuses
  - on the accelerator and user transfer line design and definition of the accelerator working points
  - beam dynamics studies of the design working point and investigation of the stability and reliability of the accelerator by means
  - The results are reported in the Conceptual Design Reports of EuPRAXIA and EuPRAXIA@SPARC_LAB, in numerous publications and will be object of the Technical Design Report of the machine

Design RMS e- beam parameters @plasma module entrance			
	Single bunch (WoP2)	Comb beam operation (WoP1)	
		Witness	Driver
Q (pC)	200 - 500	30 -50	200 -500
E (GeV)	up to 1.0	Up to 0.650 GeV	
$\Delta\gamma/\gamma$ (%)		< 0.10	
$\varepsilon_{nx,y}$ (mm·mrad)	< 1.0	0.5 - 1.0	2.0 -5.0
$\sigma_{z\text{-}rms}$ (µm)	20 - 50	< 6	< 65
$I_{peak\text{-}slice}$ (kA)	1.0 – 2.0	> 1.5	

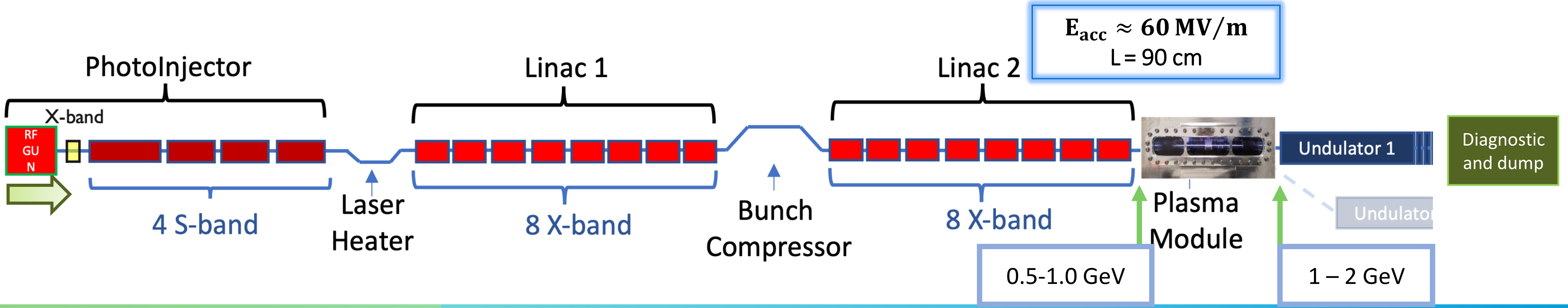

EXPECTED SASE FEL PERFORMANCES

Radiation Parameter	**Unit**	PWFA	Full X-band
Radiation Wavelength	nm	**3-4**	4
Photons per Pulse	$\times 10^{12}$	**0.1-0.25**	1
Photon Bandwith	%	**0.1**	0.5
Undulator Area Length	m	30	
ρ(1D/3D)	$\times 10^{-3}$	**2**	2
Photon Brilliance per shot	$mm^2 mrad\ bw(0.1\%)$	$\mathbf{1-2 \times 10^{28}}$	1×10^{27}

Electron Beam Parameter	**Unit**	PWFA	Full X-band
Electron Energy	GeV	**1-*1.2***	1
Bunch Charge	pC	**30-50**	200-*500*
Peak Current	kA	**1-2**	1-2
RMS Energy Spread	%	**0.1**	0.1
RMS Bunch Length	μm	**6-3**	24-20
RMS norm. Emittance	μm	**1**	1
Slice Energy Spread	%	**≤0.05**	≤0.05
Slice norm Emittance	mm-mrad	**0.5**	0.5

In the energy region between Oxygen and Carbon K-edge 2.34 nm – 4.4 nm (530 eV -280 eV) water is almost transparent to radiation while nitrogen and carbon are absorbing (and scattering)

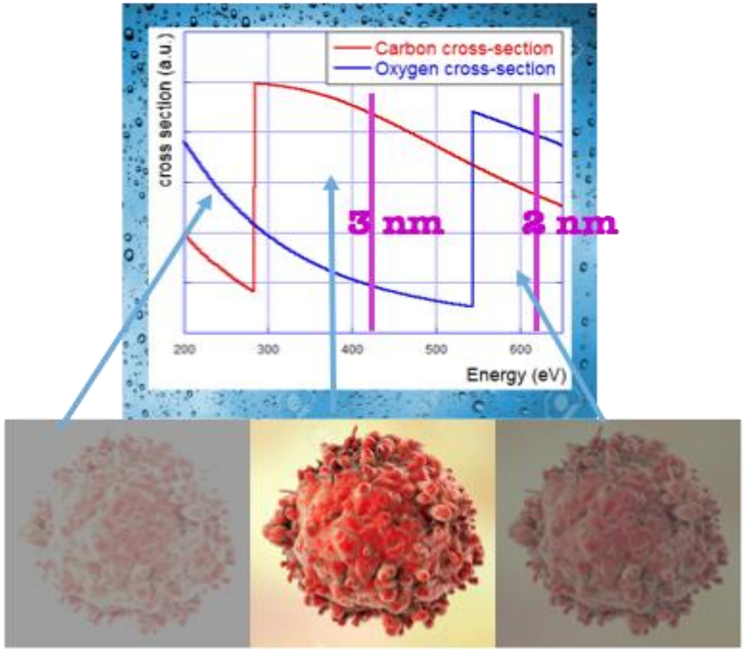

Coherent Imaging of biological samples protein clusters, VIRUSES and cells living in their native state
Possibility to study dynamics
~10 ^{11} photons/pulse needed

Courtesy C. Vaccarezza

Courtesy F. Stellato (UniTov)

Beam dynamics in a linear accelerator for PWFA

- Beside the FEL specifications, the <u>working point</u> is determined by the plasma module
  - Accelerating gradient of the order of GV/m
  - Weakly non-linear regime (bubble with resonant behaviour)

1. 200-500 pC driver + 30-50 pC witness
2. plasma density of the order of $10^{16}\ cm^{-3}$ (λ_p = 334 μm)
3. Driver-witness separation of $\lambda_p/2$
4. Driver and witness bunches of 200 fs and 10 fs rms
5. Driver and witness spot size of few μm rms with α=1

Velocity bunching technique

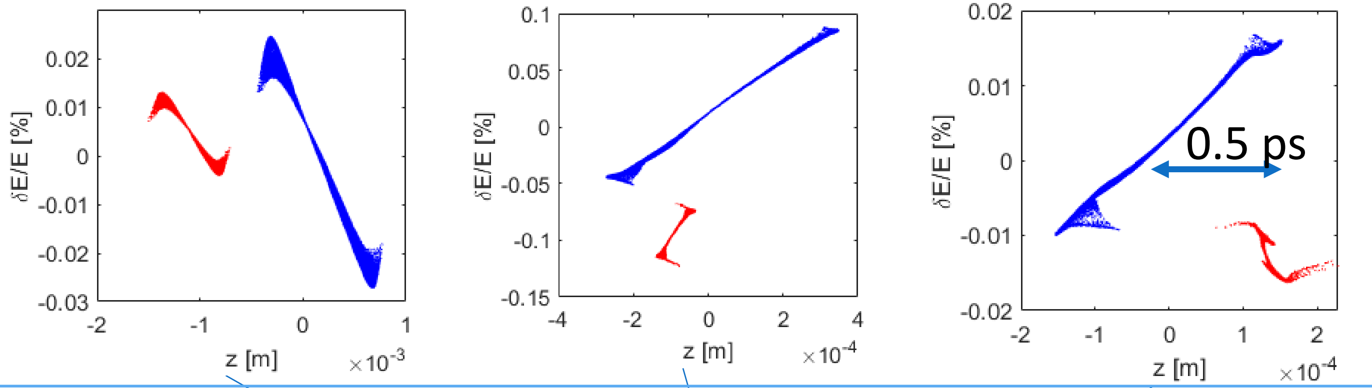

Laser comb technique

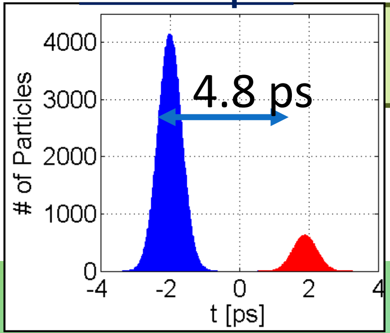

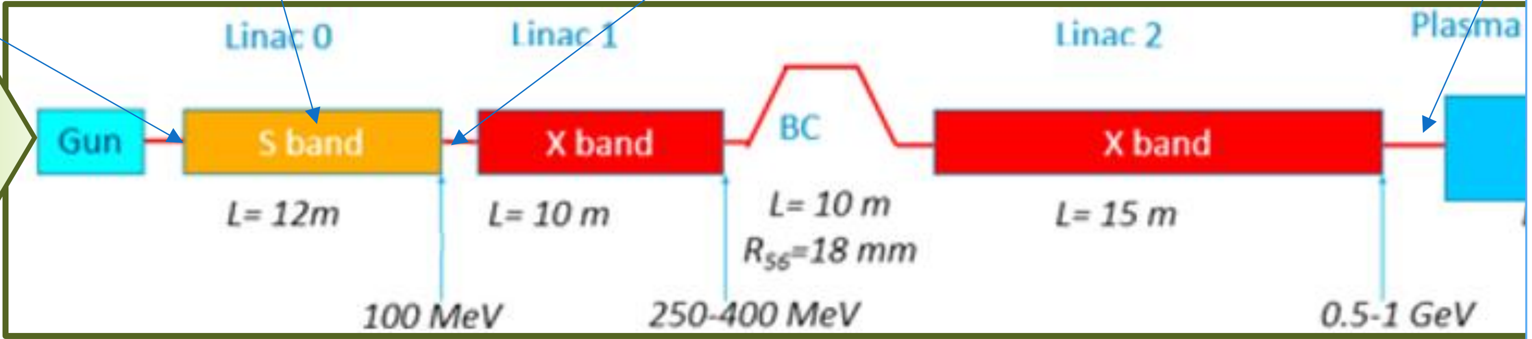

Strong focusing system

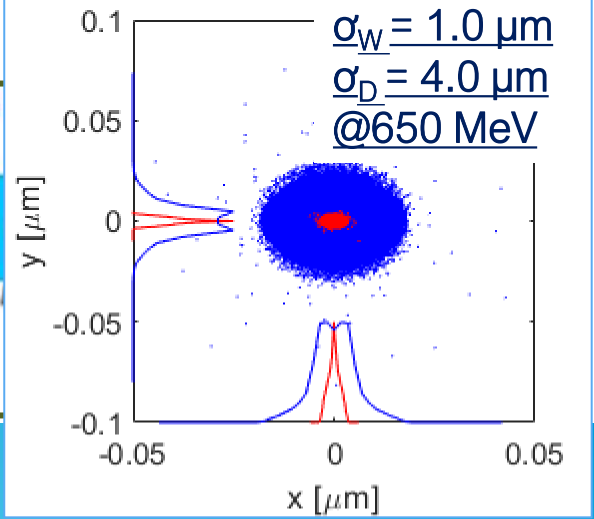

Beam dynamics studies for the design of the EuPRAXIA@SPARC_LAB accelerator: the photo-injector

- The beam dynamics has been studied by means of simulations with the TStep
  - The witness and driver distribution on the cathode has been chosen looking at the witness quality that depends on the density of the beams at the overlapping point [7]
  - Double-VB is applied in the *first and second S-band acc. structures* → this scheme ensures at same time up to 2 kA peak current and separation lower than 0.6 ps [6,11]

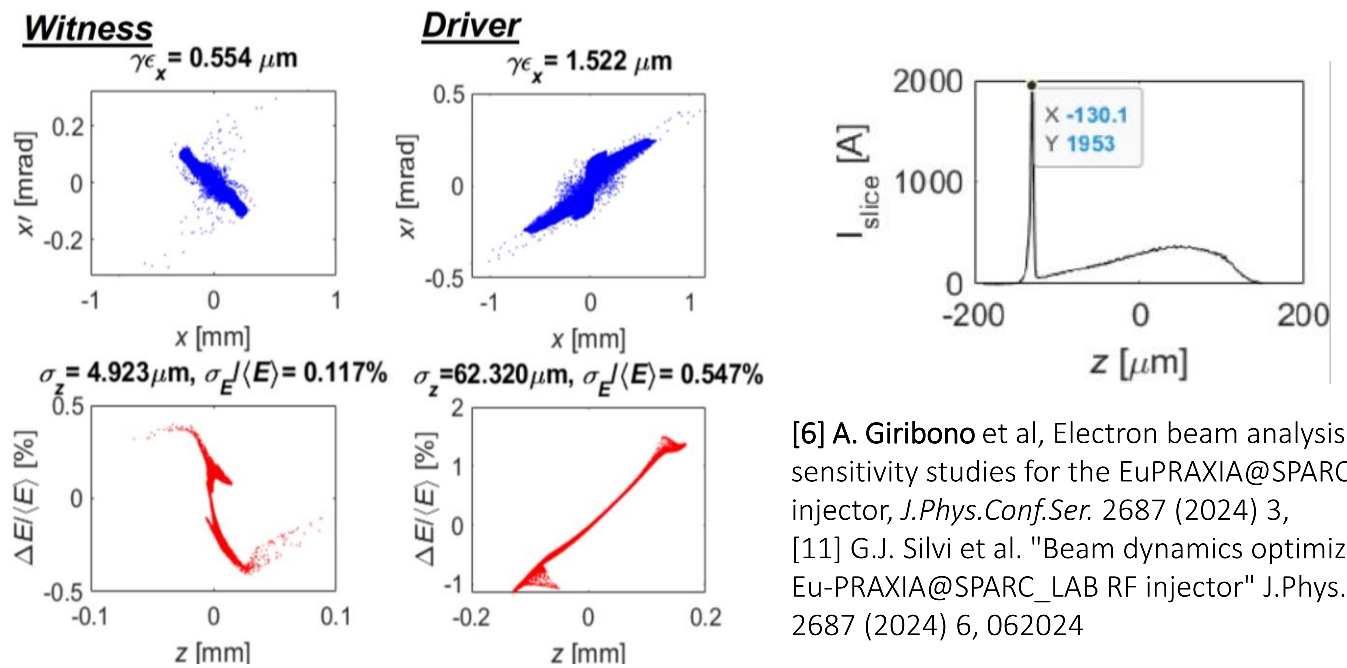

[6] A. Giribono et al, Electron beam analysis and sensitivity studies for the EuPRAXIA@SPARC_LAB RF injector, *J.Phys.Conf.Ser.* 2687 (2024) 3,
[11] G.J. Silvi et al. "Beam dynamics optimization of Eu-PRAXIA@SPARC_LAB RF injector" J.Phys.Conf.Ser. 2687 (2024) 6, 062024

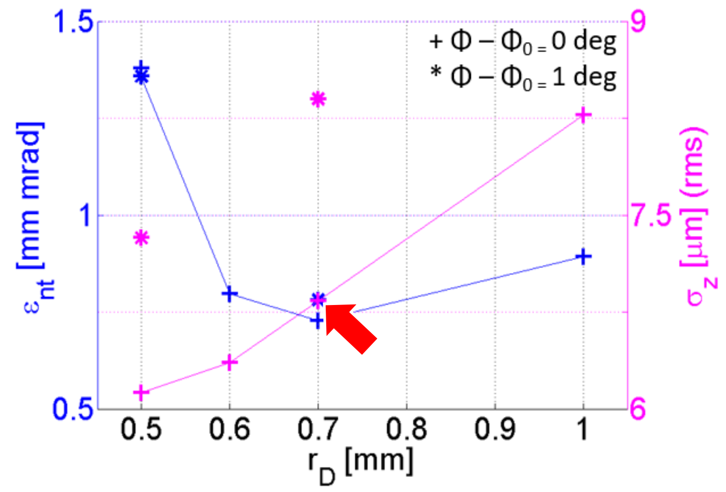

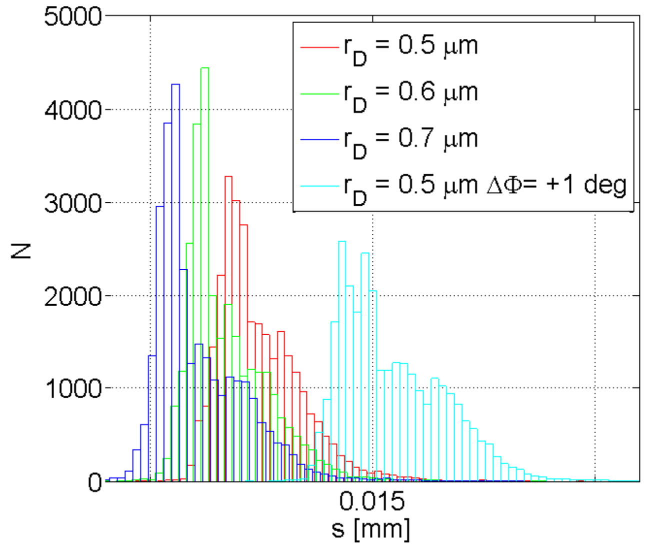

[7] A. Giribono et al. EuPRAXIA@SPARC_LAB: The high-brightness RF photo-injector layout proposal, https://doi.org/10.1016/j.nima.2018.03.0

Beam dynamics studies for the design of the EuPRAXIA@SPARC_LAB accelerator: the machine stability

Considering state of the art technology:

- ❑ Jitter on S/X-band: phase : 0.01 ps rms
  voltage: 0.02% rms
- ❑ Jitter on laser: TOA : 0.01 ps rms
  charge : ± 2 %
  Laser Spot size: ± 1%

Results of S2E simulations with TStep and elegant codes @plasma entrance. The magenta is related to the refence WP

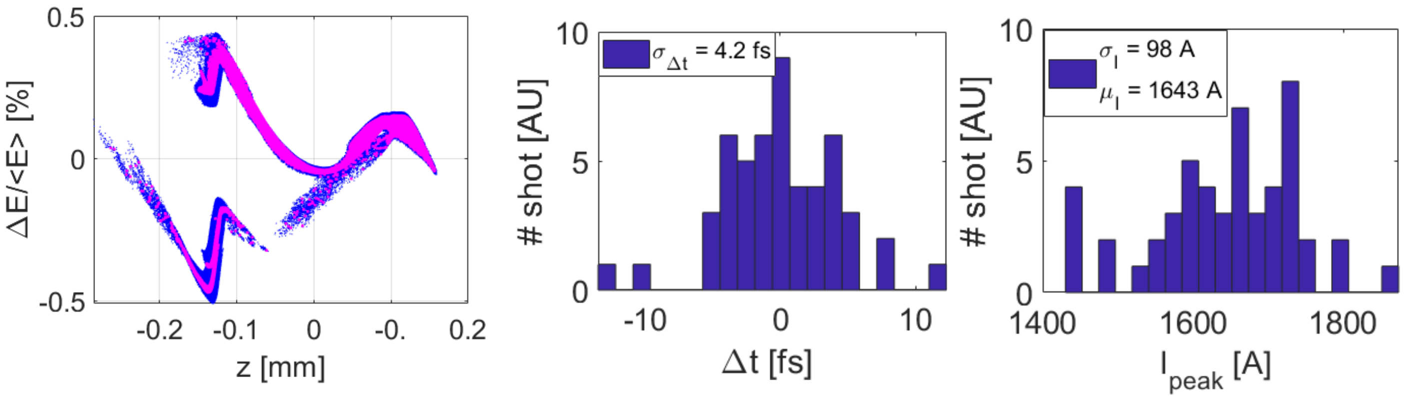

- In the worst-case scenario the emittance and the peak current are ruined of maximum 10% (still in specification)
- The most critical parameter is the witness-driver separation
  → 4.5 fs rms ↔ Energy shot to shot deviation of 1 %

Energy gain and energy spread at plasma exit vs driver-witness time distance as result of S2E sim with Architect

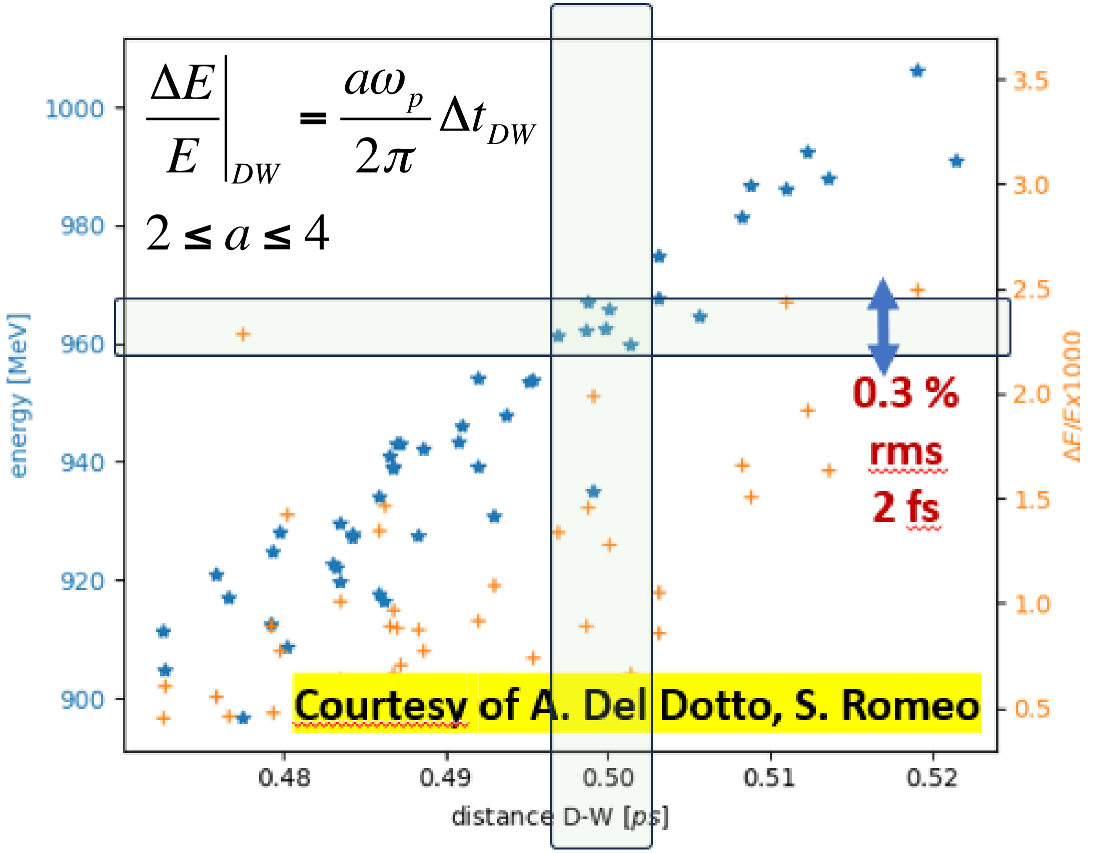

COMPLETE JITTER SIMULATIONS

- X-band accelerating structure right after the RF gun
- Sensitivity jitter study for all RF injector components in parallel with the generation of the cathode beam parameters.

Total Charge	Spot Size	Time of arrival	RF phases	Voltage
2% of the total	1% of the total	30 fs RMS	30 fs RMS	0.2% of the total

Beam parameters	w/ X-band all jitter	w/ X-band RF jitter	w/o X-band all jitter
<ε> (mm-mrad)	0.672 ± 0.031	0.676 ± 0.013	0.5710 ± 0.091
<peak current> (A)	1733 ± 230	1728± 56	1923 ± 173
<centroid distance> (ps)	0.5337 ± 0.0117	0.5462 ± 0.0048	0.5011 ± 0.0115

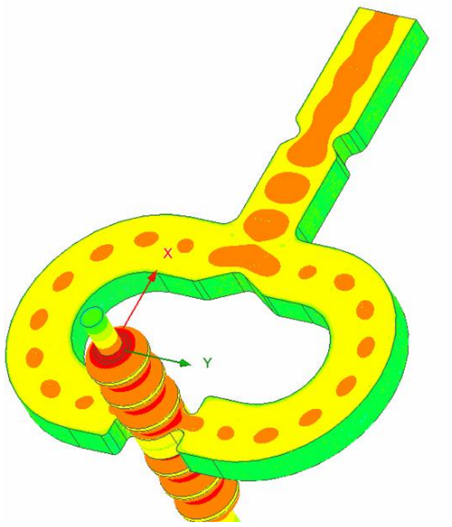

Courtesy of L. Faillace

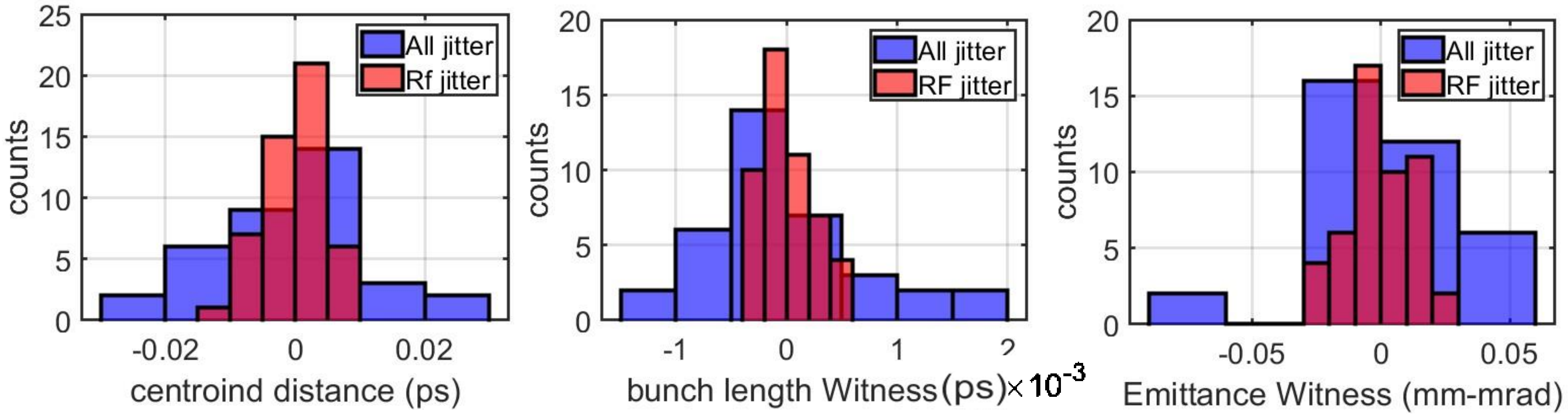

Courtesy of G. Silvi

C-BAND INJECTORS

BD studies: high repetition rate case *(conservative)*

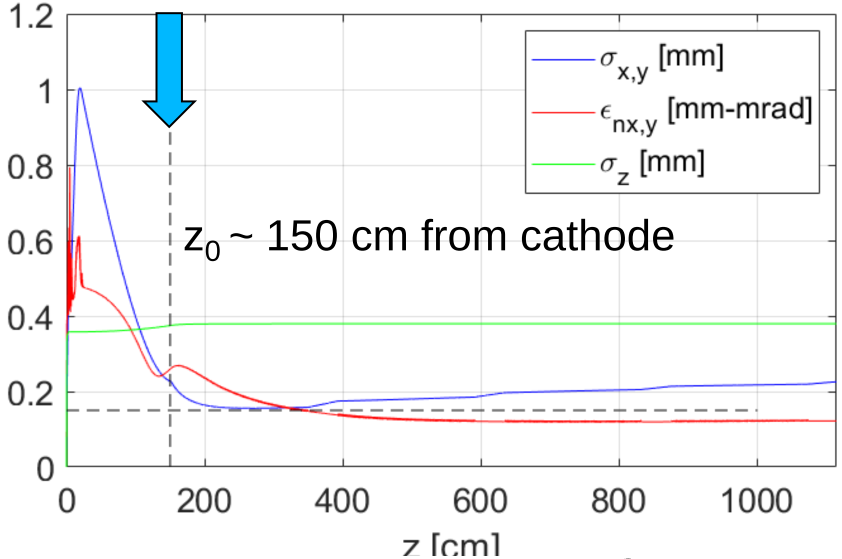

Parameters before BC1	Sim. results	Target	units
Q	75		pC
Rep. rate	1000		Hz
E	126	125	MeV
σ_E/E	0.11	0.5	%
$\epsilon_{n,rms}$	**0.12**	**0.15**	**µm**
σ_z	380	380	μm
I_{peak}	20	20	A

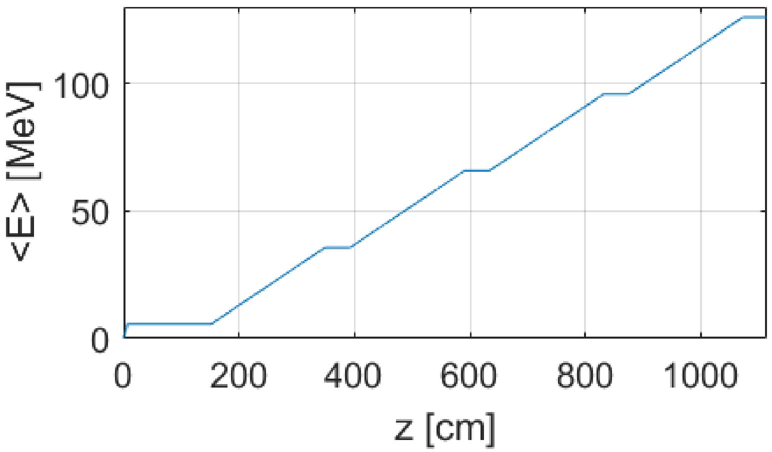

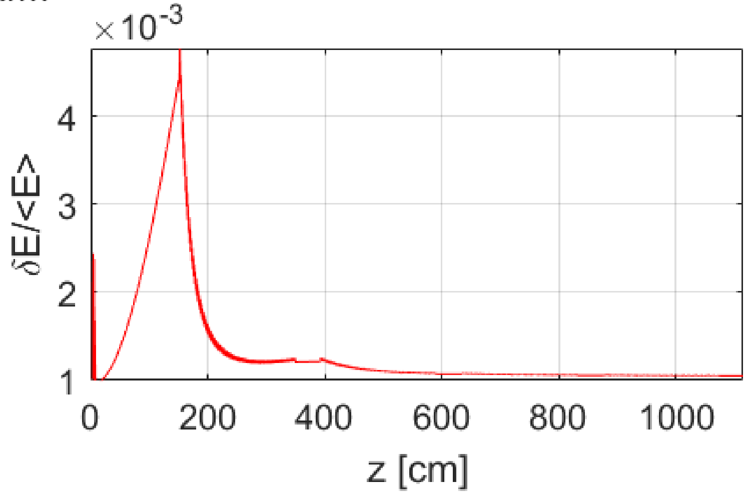

THE BOOSTER LINAC

- The booster linac design started from the Swiss FEL CDR

Fig. 2.1.1: Schematic of the SwissFEL Accelerator and FEL with the simulated beam parameters for the 200 pC operating mode.

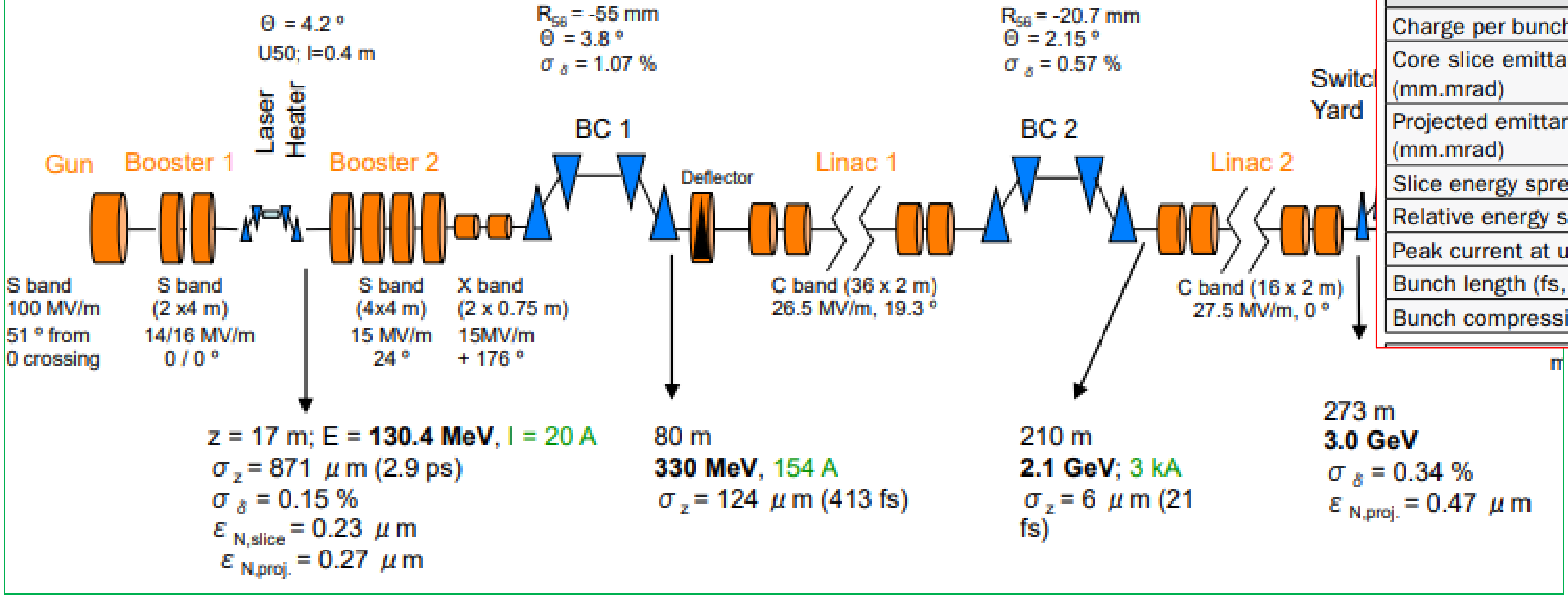

Table 1.4.2 Expected Performance of Linac, Aramis and Athos lines. Performances for different operation regimes are detailed in Chapter 2.

Design parameters for the electron beam	Operation Mode	
	Long Pulses	Short Pulses
Charge per bunch (pC)	200	10
Core slice emittance (mm.mrad)	0.43	0.18
Projected emittance (mm.mrad)	0.65	0.25
Slice energy spread (keV, rms)	350	250
Relative energy spread (%)	0.006	0.004
Peak current at undulator (kA)	2.7	0.7
Bunch length (fs, rms)	25	6
Bunch compression factor	125	240

[8] https://www.psi.ch/sites/default/files/import/swissfel_old/CurrentSwissFELPublicationsEN/SwissFEL_CDR_V20_23.04.12_small.pdf

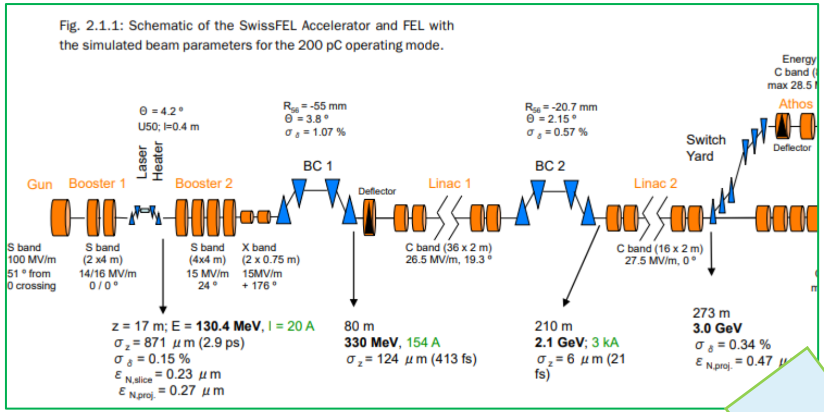

- The booster linac has been simulated with the Elegant code considering longitudinal space charge, CSR and wakefields
- It is operated off-crest to
  - Set the desired energy spread at chicane entrance
  - Minimize of the final beam energy spread
- A certain number of matching quadruples and steering have been used to carry the beam at the FEL entrance and to proper match the beam at the LH, BC1 and BC2 entrance (no emittance dilution)

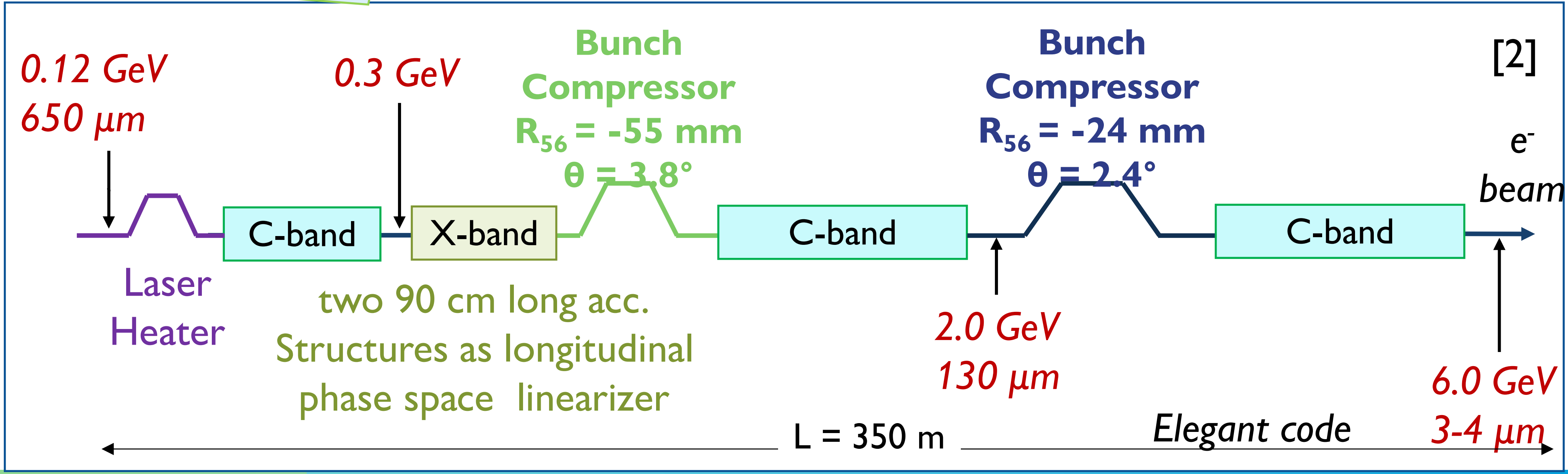

A simple matching has been adopted to proper match the beam at

the Linac section entrance to transport it through the linac

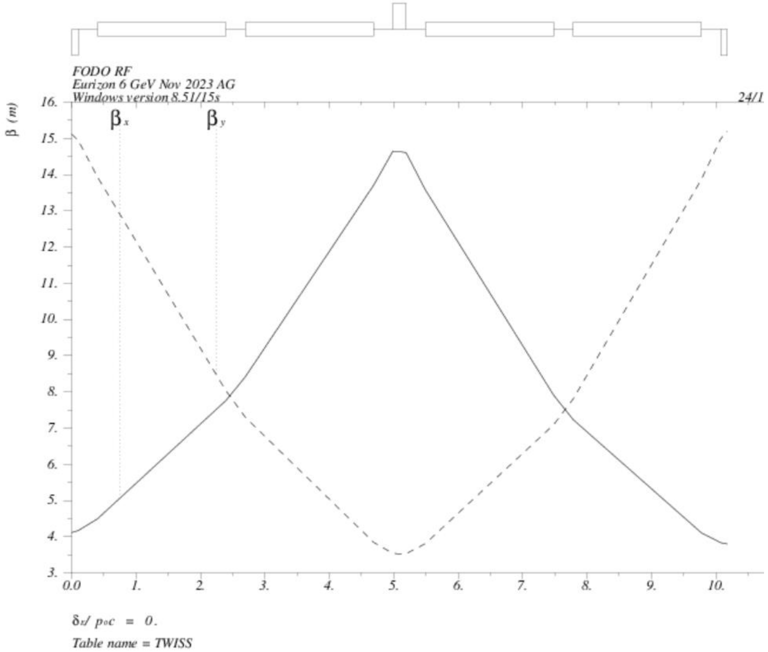

the LH, BC1 and BC2 entrance (no emittance dilution)

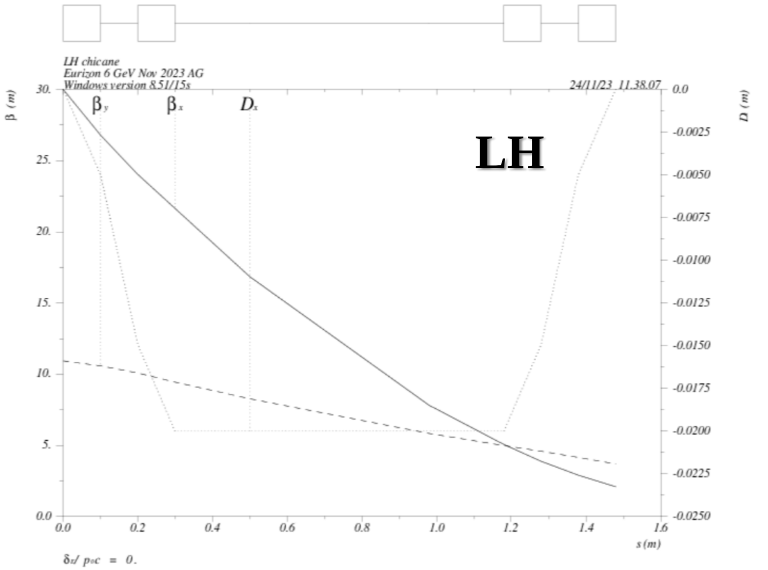

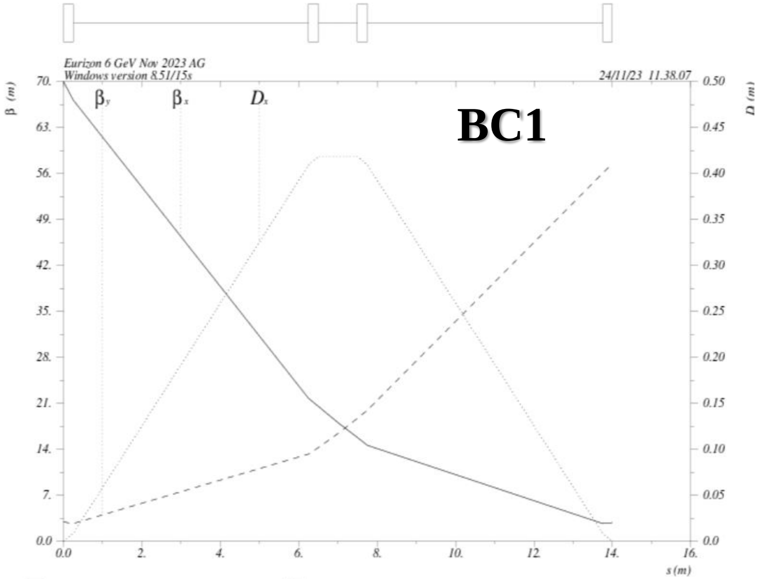

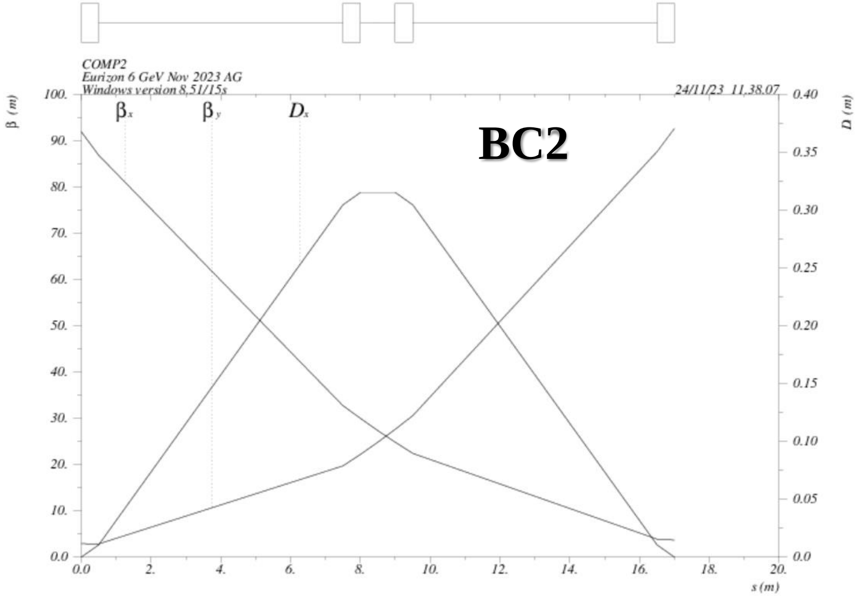

Effects of the linearization

Simulated with elegant (500k particles)

Fig.7 – Beam longitudinal phase space.

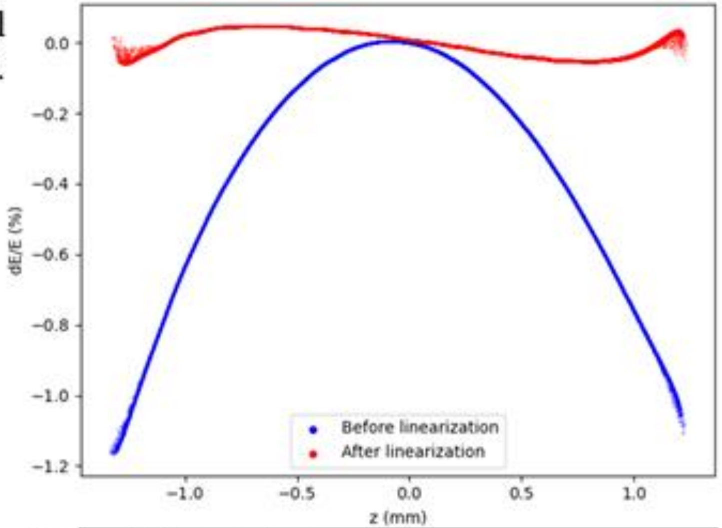

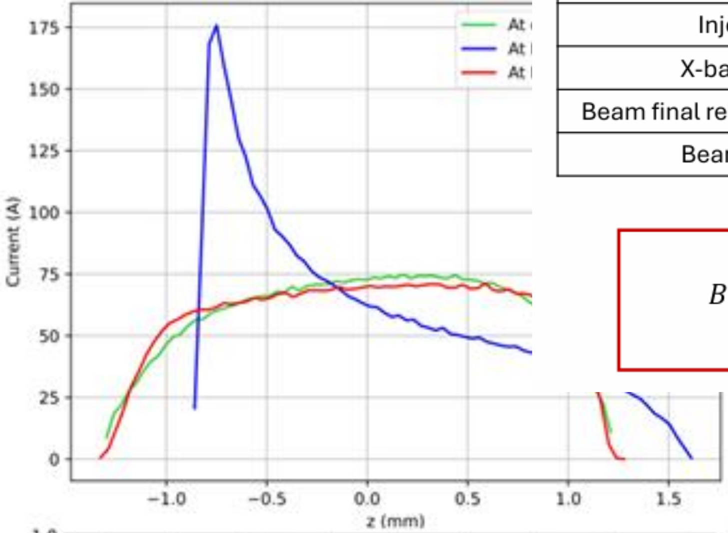

Tab. 3 – X-band cavity parameters

Parameter	Value
X-band resonant frequency [GHz]	11.424
Rep. rate [kHz]	0.1
X-band cavity field [MV/m]	92.4
Injection phase [deg]	179.72
X-band cavity length [m]	0.5
Beam final relative energy spread, rms [%]	0.03
Beam final energy [MeV]	145

$$B = \frac{Q}{\varepsilon_{nx}\varepsilon_{ny}\sigma_t\sigma_E} \approx 10^{18}\ [\mathrm{A/m^2}]$$

Fig. 9 – Relative energy distribution.

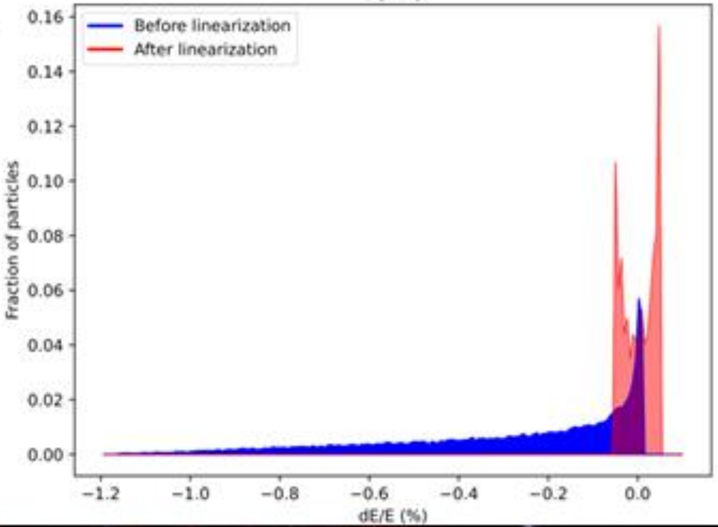

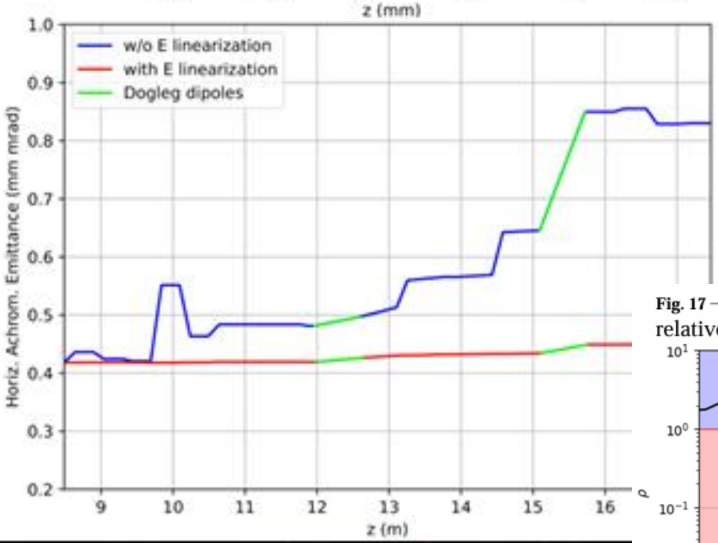

Fig. 10 – Horizontal achromatic emittance evolution.

Fig. 17 – Laminarity parameter along the beamline, measuring the relative importance of space charge effects vs. emittance pressure.

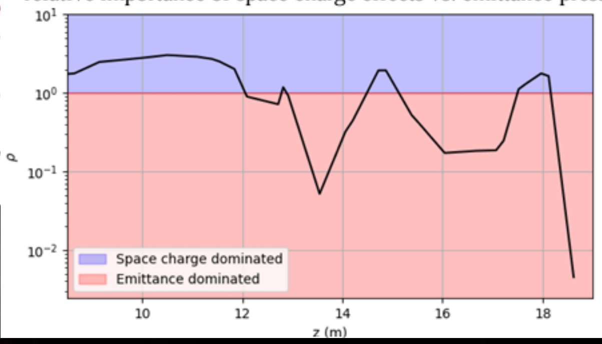

Bunch Selection Module (BSM)

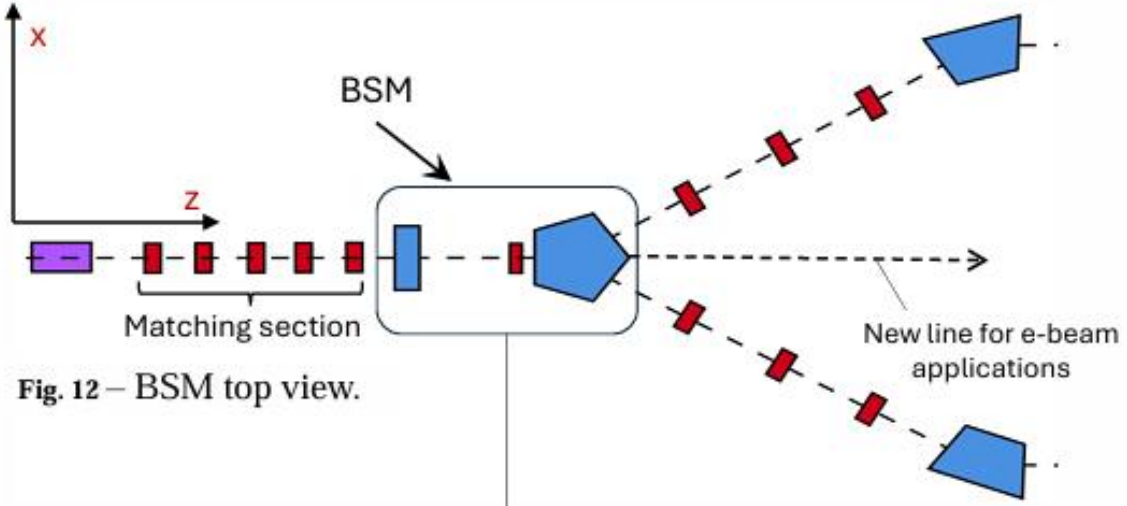

Fig. 12 – BSM top view.

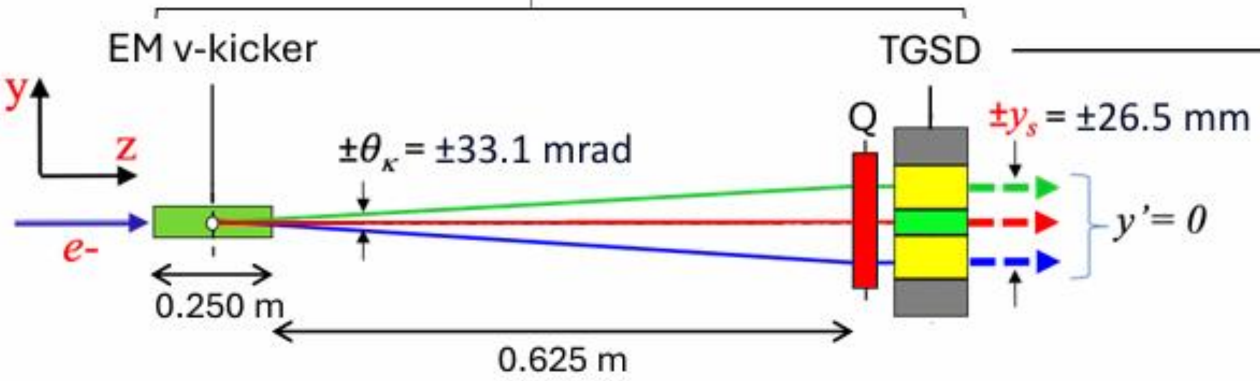

Fig. 13 – BSM side view.

Multimode operation

BSM scheme provides the possibility to select the beamline on a bunch-by-bunch basis, allowing a quasi-simultaneous operation of up to three user areas.

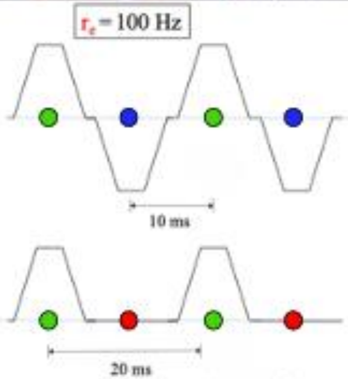

Fig. 15 – Examples of possible deflecting patterns.

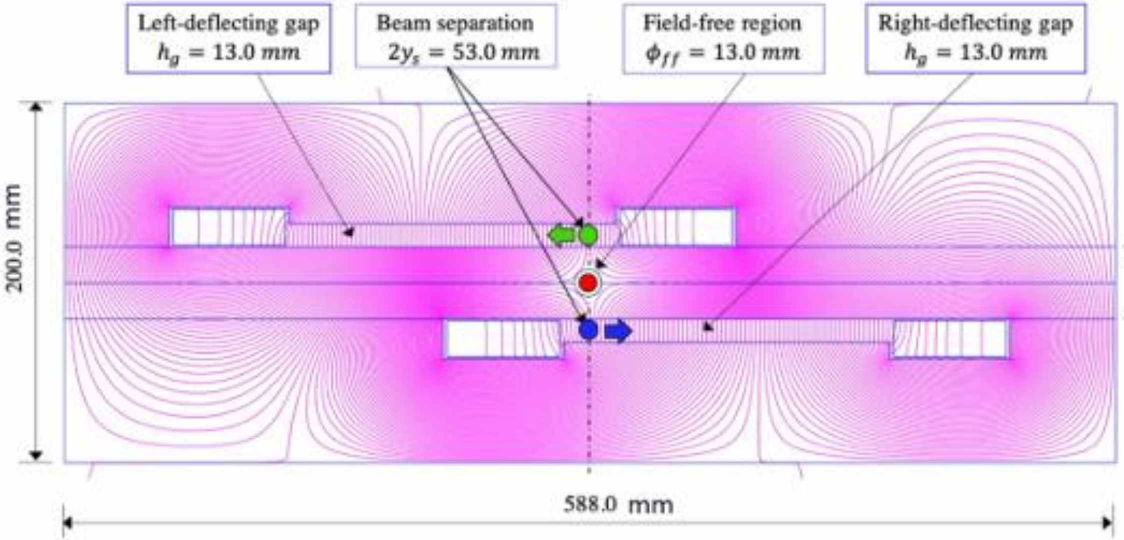

Fig. 14 – Front view vertical section of the Poisson-optimized Twin-Gap Septum Dipole (TGSD).

Dispersion contribution to the projected emittance

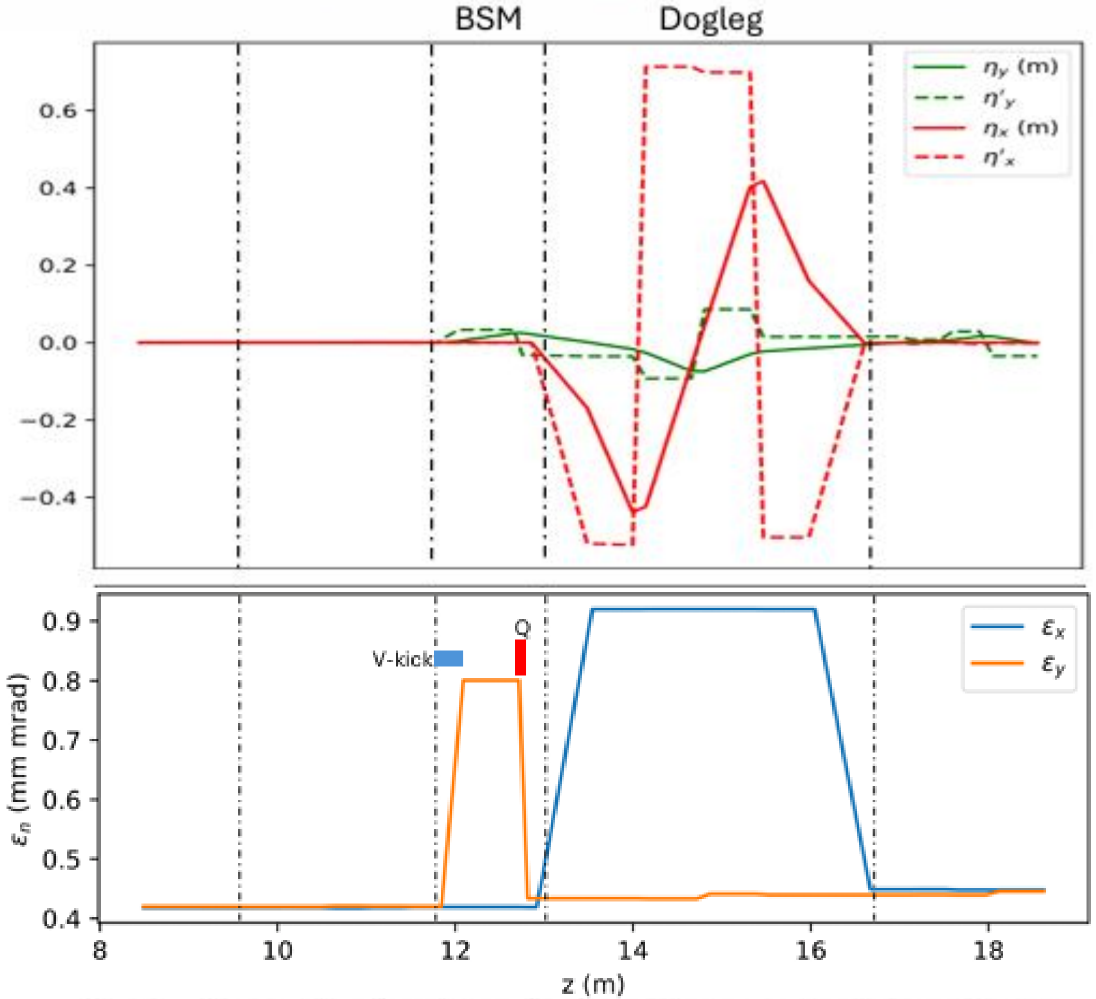

Fig. 20 – Dispersion functions (top) and beam projected emittance (bottom) along the beamline.

Chromatic $\mathcal{H}$-function

$$\gamma\eta^2 + 2\alpha\eta\eta' + \beta\eta'^2 = \mathcal{H}$$

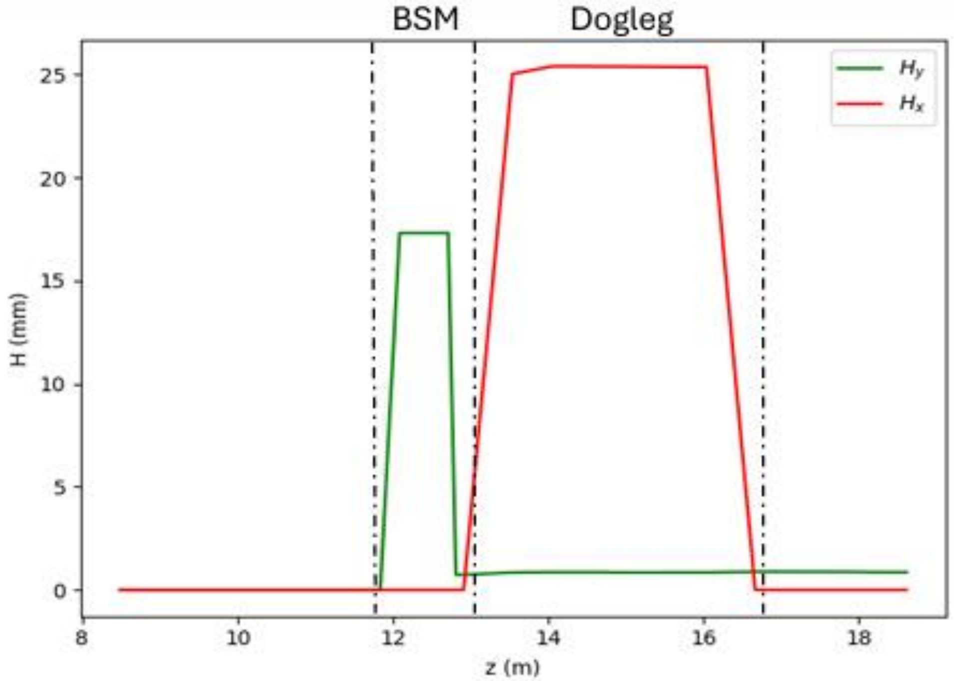

Fig. 21 – $\mathcal{H}$-functions along the beamline.